Cretaceous Pab Reservoir Quantitative Interpretation And PNN Estimation Of Petrophysical Properties For Hydrocarbon Assessment Using Integrated Well And Seismic Data.

BY

TOUQEER KHAN

02112011011

M.PHIL GEOPHYSICS

2020-2022

DEPARTMENT OF EARTH SCIENCES

QUAID-I-AZAM UNIVERSITY ISLAMABAD,

PAKISTAN

CERTIFICATE

This dissertation is submitted by **TOUQEER KHAN** S/O **TARIQ KHAN** is accepted in its present form by the Department of Earth Sciences as satisfying the requirement for the award of M.Phil degree in **Geophysics.**

RECOMMENDED BY

Prof. Dr. Mona Lisa _____

(Supervisor)

Dr. Aamir Ali _____

(Chairman Department of Earth Sciences)

External Examiner _____

ACKNOWLEDGEMENT

In the name of **Allah** the most merciful and most beneficent. All praises to Him who is Almighty, The One, The Everlasting, Who begets none, is be gotten, by no one, and there is none His equal. Alhamdulillah. I bear witness that Holy Prophet **Muhammad (PBUH)** is the last prophet of Allah, whose life is perfect model for the whole mankind till the Day of Judgment. I am thankful to Allah for the strengths and His blessing in completing this thesis.

I am nothing without your help. Please keep me always in prostration before you and let me not leave before anyone except you.

Foremost, I would like to express my sincere gratitude for my supervisor **Prof. Dr Mona Lisa** for her continuous support throughout my M.Phil. study and research and for her motivation, enthusiasm, immense knowledge and confidence in me. I learned from her insight a lot. Her guidance helped me in all the time of research and writing of this thesis. I could not have imagined having a better advisor and mentor for my study.

I am extremely thankful to all of my teachers for their endless love, prayers and encouragement and my special appreciation to those who indirectly contributed in this research.

TOUQEER KHAN

Dedication

I would like to dedicate this research work to my Father and Mother whose affection, love, encouragement and prays of day and night make me able to get such success and honor. Along with all hard working and respected Teachers

Abstract

Seismic reflection is an indirect geophysical tool for hydrocarbon exploration that is commonly employed. The main goal is to characterize physical reservoir parameters and evaluate hydrocarbon reservoirs. The use of seismic amplitude in conjunction with wireline logs aids in the estimation of these crucial reservoir parameters. The major goal of this research is to improve reservoir characteristics assessment in the sands of the Pab formation in the Zamzama Gas Field in Pakistan's Lower Indus Basin. Seismic interpretation, wireline log analysis, seismic inversion techniques and Probabilistic Neural Network (PNN) are used to achieve the goals.

The database has a very significant role in the project. In our study area, the data is used to estimate the study purpose i.e. 3D seismic interpretation, petrophysics, inversion, and PNN etc. For detiled studies I used ten lines i-e five seismic inlines (inline 450,460,470,480, and 470) and five seismic crossline (crossline 1360,1370,1380,1390,1400) along with two well i-e Zamzama 03 and 05.

Because the Zamzama gas field is located in the Lower Indus Basin, which has a compressional regime, the structure identified here is a thrusted anticline. Three horizons, Khadro , Pab, and Fort Munro are marked on a synthetic seismogram. Faults are being indicated along with the distortion or discontinuity with an eastward-facing N-S thrust fault. Our subsurface structures were also validated by time and depth contour maps.

Petrophysical analysis of borehole log data is used to evaluate reservoir parameters. At Zamzama well 03 and 05 the Pab formation is classified as a reservoir that meets all of the requirements for a reservoir. According to petrophysical data, the Pab formation has a high effective porosity of 10-16 percent, a low volume of shale of 6-10 percent, and a hydrocarbon saturation of 70-87 percent. The reservoir lithology is proven using well Zamzamz 03 by facies analysis, which is the cross-plotting of different logs such as Neutron vs Sonic logs. These tests are carried out at the reservoir level, revealing that the reservoir's principal lithology is sand with thin shale sequences interbedded.

The reservoir location is confirmed using seismic Model-based inversion (MBI). Pab sandstone has a low impedance value on the inverted seismic section, which could be a significant indicator of hydrocarbon content.

Model-based inversion (MBI) are used to choose low impedance zones with a high correlation coefficient and low error. At the reservoir level, MBI has a correlation coefficient of (0.99) and an error of (0.045). Inversion algorithm strategies resolve the reservoir well, however, MBI outperforms them all in terms of maximum correlation and smallest error in the research region.

And last we perform Probabilistic Neural Network (PNN) to predict seismic reservoir properties from well log data and seismic attributes by using Hampson Russell software .

Contents

CHAPTER #1
INTRODUCTION TO STUDY AREA

1.1 Study Area Reveiw:

This dissertation uses 3D seismic interpretation and Seismic Colored Inversion (SCI) techniques to better comprehend the geophysical and geological characteristics of the Zamzama block concerning hydrocarbon exploration and production. The Zamzama Block is around 200 kilometers north of Karachi in Pakistan's Sindh Province. This field has a total size of 129 square kilometers. It is a BHP Petroleum concession block that was discovered in the year 2000. (Dorn 1998).

Pakistan's southern and northern regions have a lot of hydrocarbon potential (Qadri, 1995). The Lower Indus Basin has served as a potential zone for recovering a significant amount of hydrocarbon (Qadri, 1995). The Zamzama gas field is located 200 kilometers north of Karachi in the Sindh region of Pakistan's Kirthar fold Belt. The Zamzama gas field is shown in Figure 1.1. It has a surface area of 120 square kilometers and is Pakistan's fourth discovered gas deposit (Jackson et al., 2007). It's the eastward progressing thrusted anticline with a huge north-south oriented.

In the kirthar fold belt, the late cretaceous Pab sandstone serves as a primary reservoir, whereas in the zamzama gas field, it serves as the main reservoir. Bhit (southwest of zamzama) and kadanwari, sawan, and maino fields (northeast of zamzama) are some other gas fields near the area.

The entire known recoverable reserves from the core area of the zamzama field are estimated to be 1.7 Tcf of gas (Jackson et al., 2007). For the next 10 to 12 years, the field will produce roughly 320mmcf/d of gas and 2000 standard barrels of condensate (stb/d), with an economic field life of 15 to 25 years. The zamzama gas is dry and sweet, with a condensate value to gas ratio of 6.5 barrels per million cubic feet (Jackson et al., 2007) .

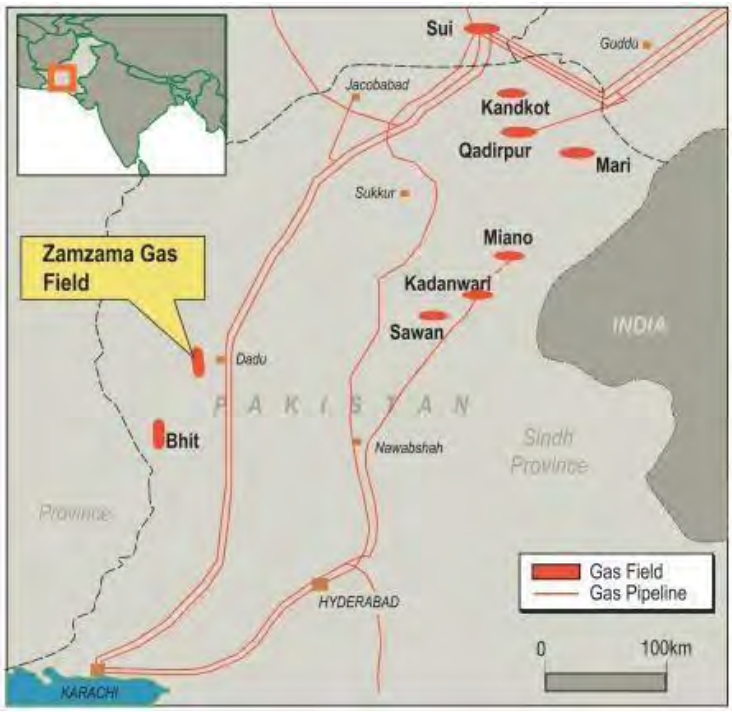

Figure 1.1 Major discoveries in southern indus basin including zamzama gas field (Bhpbilliton, 2003).

1.2 Research overview:

Exploration geophysicists began working on the seismic approach in 1915, and it has since been shown to be quite beneficial for imaging subsurface geological features and locating structural or stratigraphic traps (Coffeen, 1986). Seismic surveys, which portray data as a time series of reflections through the subsurface, are commonly used in hydrocarbon exploration (Badley 1985).

Since 1920, the seismic reflection method has played an important role in exploration. The seismic method is a popular remote sensing technique for imaging subsurface layers at depths ranging from a few meters to kilometers. The basic concept is to generate an acoustic wave from a single source. This wave travels into the earth's subsurface, where it partially refracts and reflects due to lithological differences in acoustic impedance. The set of localized receivers on the surface records refracted and reflected seismic waves (Bust, 2013).

The primary tool for hydrocarbon exploration is 3D seismic interpretation. It is carried out on the seismic cube of a gas field with sand reservoirs. 3D seismic surveys offer numerous benefits and can be used for a wide range of concerns, from exploration to development. They're also useful for limiting the scope of extensive reservoir characterization. The fundamental concept is to represent

the subsurface structure as a simple model with resolvable parameters (Dorn, 1998). In less disturbed places, seismic interpretation is usually a quick procedure, but in geologically complex locations, such as zones of the low impedance, it can be slow and cautious. Then, based on this, contour maps of overlying sand reservoirs are created.

The study of rock characteristics and their interaction with fluids is known as petrophysical analysis (Rider, 1995). The most significant attribute of fluid for its storage and movement within the rock is porosity and permeability (Donaldson, 2015). The majority of data comes from petrophysical records, so they are employed in the mapping and identification of lithologies . The deposition environment influences mineralogical properties of rock such as sorting, compaction, cementation, and grain size (Donaldson, 2015).

Lithology and thickness, color, composition, grain characteristics, bedding characteristics, sedimentary structures, type of overlaying and underlying contacts, trace and body fossils, and post-depositional features are all considered in the facies study (Rider, 1995). The facies analysis of distinct logs is used to confirm the lithology of the reservoir. Facies are sedimentary bodies that are distinguishable from surrounding deposits formed in different depositional conditions.

Seismic inversion is the primary tool used by geophysicists to better understand the subsurface. The information from well logs is extended to seismic volume through inversion. Different types of seismic inversion are employed to solve different challenges (Barclay et al. 2007). Seismic inversion is used to recover rock physical attributes from seismic data and provides a complete image of subsurface geology. It is used to resolve seismic data and characterize reservoirs at various levels (Barclay et al. 2007).

Because of the inversion algorithm, seismic colored inversion (SCI) alters the spectrum shape of the seismic data. Different physical properties of seismic waves were placed against each other to determine the project area's petroleum potential. The impedance fluctuations are plotted against two-way time (TWT),and the amplitude and frequency plots are interpreted in an acoustic impedance log of spectrum analysis. The data is analyzed in the acoustic impedance domain using seismic colored inversion on a 3D seismic cube.

Inversion is a technique for predicting, calculating, and inferring physical properties from actual data (Sen., 2006). This resulted in more accurate estimates of reservoir parameters like as porosity,

water saturation, volumetric, and so on. Another feature of inversion is the estimation of risks and uncertainties (Pendrel, 2000). As a result, the various inversion techniques can be useful in reservoir management and development.

1.3 Geographical Boundries:

The Zamzama field is surrounded by the Kirthar range in the west, which consists of a 560 km long and 130-220 km wide belt with an NS direction, containing basins and valleys, while Sukkur is in the NE and district Hyderabad is in the SE, the river Indus is in the east, and Karachi is in the south. As seen in Figure 1.2, Lake Manchor is located in the south near the Indus River, which flows east.

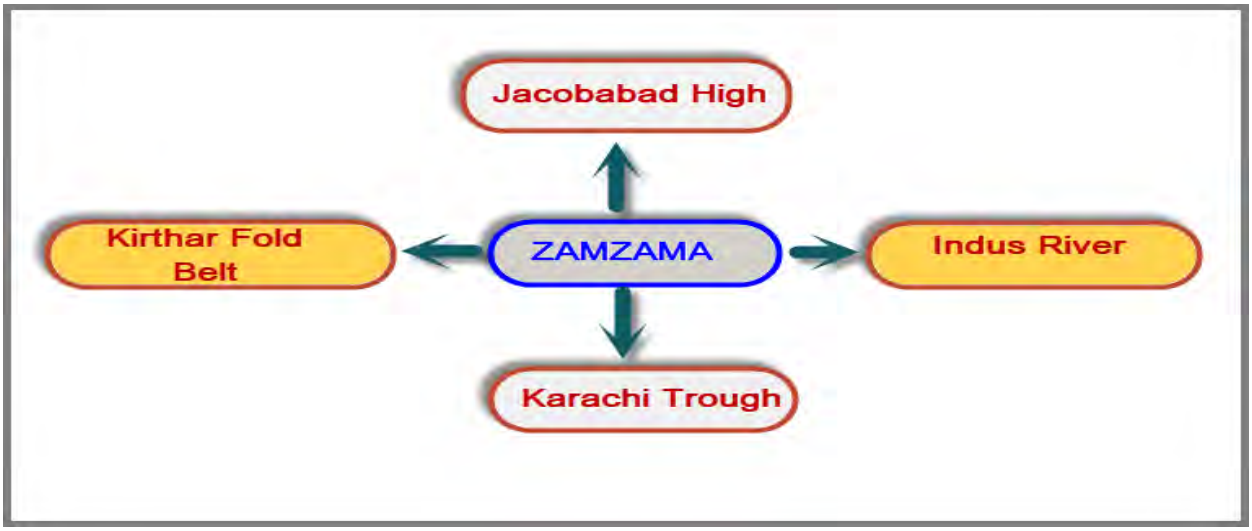

Figure 1.2: Geographical boundaries of Zamzama Gas Field.

1.4 Data Description:

The database has a very significant role in the project. In our study area, the data is used to estimate the study purpose i.e. 3D seismic interpretation, petrophysics, inversion, and PNN etc. The data is acquired from the LMKR through permission from the Department of Earth Science Quaid-i-Azam University Islamabad, after receiving approval from DGPC (Directorate General of Petroleum Concessions).

1.4.1 Seismic data:

Table 1.1 Showing In-lines and Cross-lines information.

Lines	Start	End
In-line	411	516
Cross-line	1319	1449

1.4.2 Well data:

Well log data is presented in las format. There are three wells in the data set: zamzama-03, and zamzama-05. The table below contains a detailed description of each well.

Table 1.2 Wells Information of Zamzama Gas field.

Sr.no	Well name	Latitude	Longitude	Total depth	Well type	Final status
1	Zamzama-03	26.7138	67.6682	3698	Development	Gas
2	Zamzama-05	26.6676	67.6706	3871	Development	Gas

1.5 Base map:

Kingdom software (IHS) is used to input 3D seismic data, and a base map is created.

The base map depicts well locations, concern boundaries, seismic survey line direction, and survey shot positions. Latitude and longitude or Universal Transverse Mercator (UTM) grid information is the geographic reference on the base maps which contain the cultural data of roads and buildings. . Topographic maps are used as a base map for surface geological information.

The base map in geophysics shows the alignment of seismic lines and the locations where seismic

data was collected (Sen., 2006). The base map depicts the locations of all inline, crosslines, and wells. Inline lines vary along the x-axis, while cross lines vary along the y-axis. On the seismic cube, Zamzama-03 and Zamzama-05 are placed. Figure 1.3 depicts the research area's base map, which includes all lines and two wells.

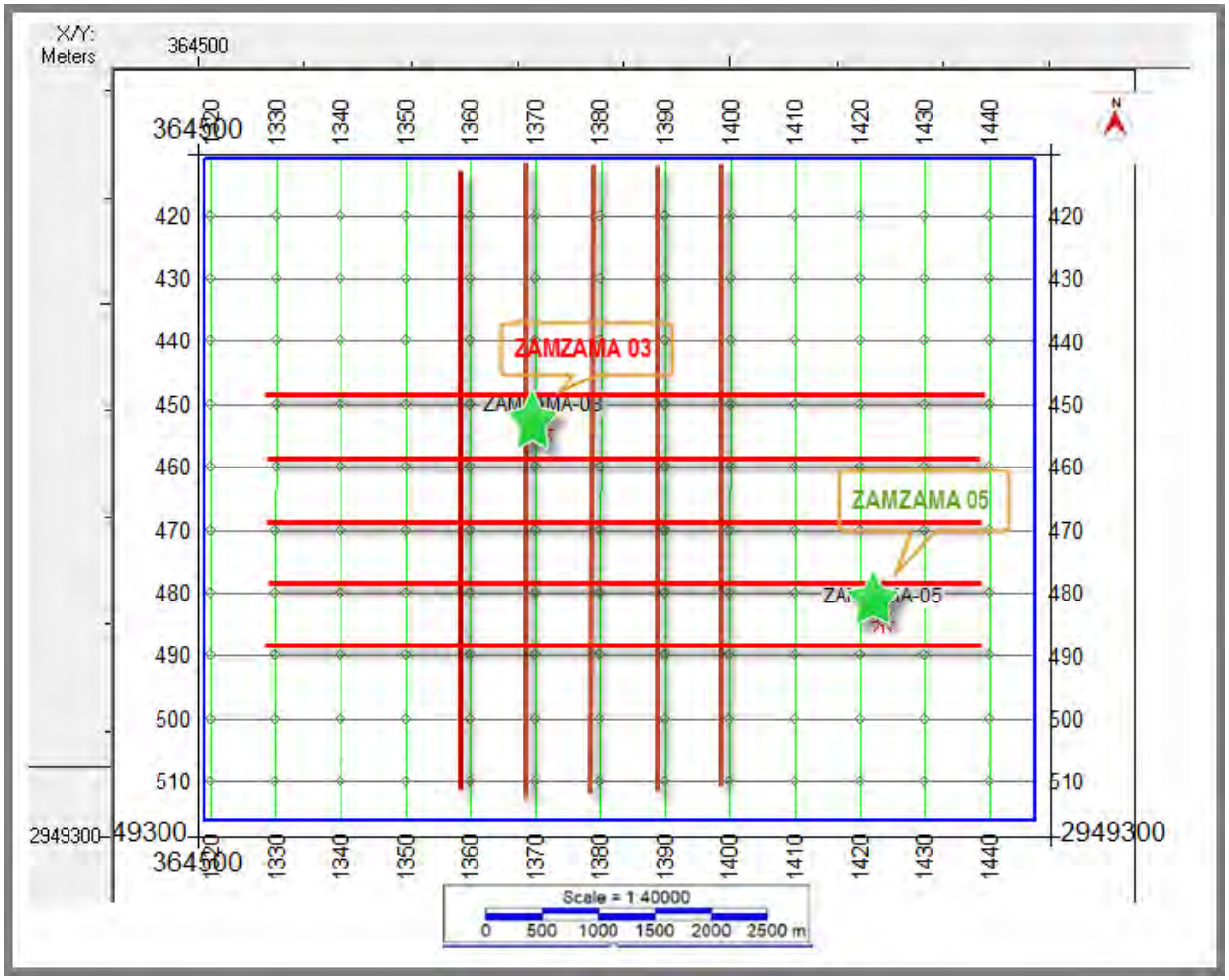

Fig 1.3: Basemap of study area..

1.6 Objectives:

1. Use 3D seismic interpretation to better understand the structural and topographical patterns of selected reservoirs for hydrocarbon accumulation and trapping mechanisms for field development reasons.

2. Identification of suitable structures for hydrocarbon accumulation using detailed 3D seismic structural interpretation.

3. Petrophysics examines digital well log data to identify and assess hydrocarbon-bearing zones in the Goru sands.

4. Evaluate reservoir parameters to identify hydrocarbon zones in the research area.

5. Perform a seismic post-stack colored inversion to look at the variation of acoustic impedance at the reservoir level.

1.7 Workflow of research:

Figure 1.4 illustrates the research workflow.

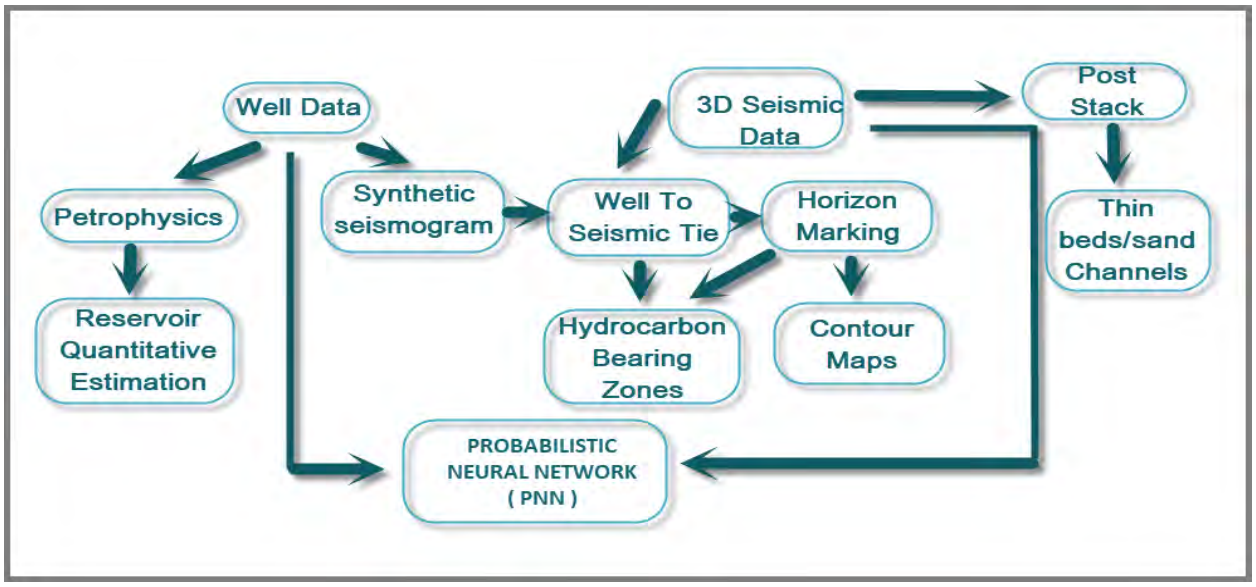

Figure 1.4: Workflow of Research

CHAPTER#2
GEOLOGY AND TECTONICS OF STUDY AREA

2.1 Introduction:

The geology of the study area plays an important role in seismic and stratigraphic interpretation (Bacon, Simm, & Redshaw, 2003). Geophysicists must familiar with the geology of the area and regional geology for precise seismic interpretation (E.Badley, 1987).

The Zamzama block is located in the Kirthar Sub Basin, which is a sub-part of the Southern Indus Basin, and Southern Indus Basin is a sub-basin of the Lower Indus Basin. The Zamzama block's geographical and Basinal location, petroleum history, tectonic, geological setting, depositional environment, structural style, stratigraphy, and petroleum system are all studied in detail.

2.2 Geological Setting:

Hydrocarbons, migration, and entrapment are all controlled by the geological environment of a sedimentary basin. According to Kazmi and Jan, Pakistan's geology is separated into two domains: Gandwanian and Tethyan. The Indo-Pak crustal plate supports the southern half of this, which is part of the Gandawain domain.

This area has rocks dating from the Triassic to the Recent epochs. The formation is made up of sand masses that have formed in a variety of shallow marine environments, spanning from the coast face to the lower shelf. During the late Cenozoic, the greater influence of clastic materials from the north drives the sea to withdraw to the south. The Indus basin was filled with sediments by the end of the Paleocene, and it resembled a large flood plain with braided streams, with the folded belts providing the sole height. During the Cretaceous, the Indian plate drifted and rifted, resulting in the formation of the Lower Indus Basin. Sedimentary sections from the Tertiary to Mesozoic epochs show appropriate source, reservoirs, and cap rocks.

2.3 Location:

The Zamzama field lies 200 kilometers from Karachi in the Sindh province of Pakistan's Dadu district. It is surrounded by Kirthar mountain ranges in the west and Sukker in N-E Hyderabad district in S-E, Indus River in east and Karachi in the south, Manchor Lake is in just south of area near to Indus River, Kirhter Mountains in the west. The Zamzama Block is 560 kilometers long

and 130-120 kilometers broad. Figure 2.1 depicts the research region, which is located in the center and southern Kirthar Fold Belt.

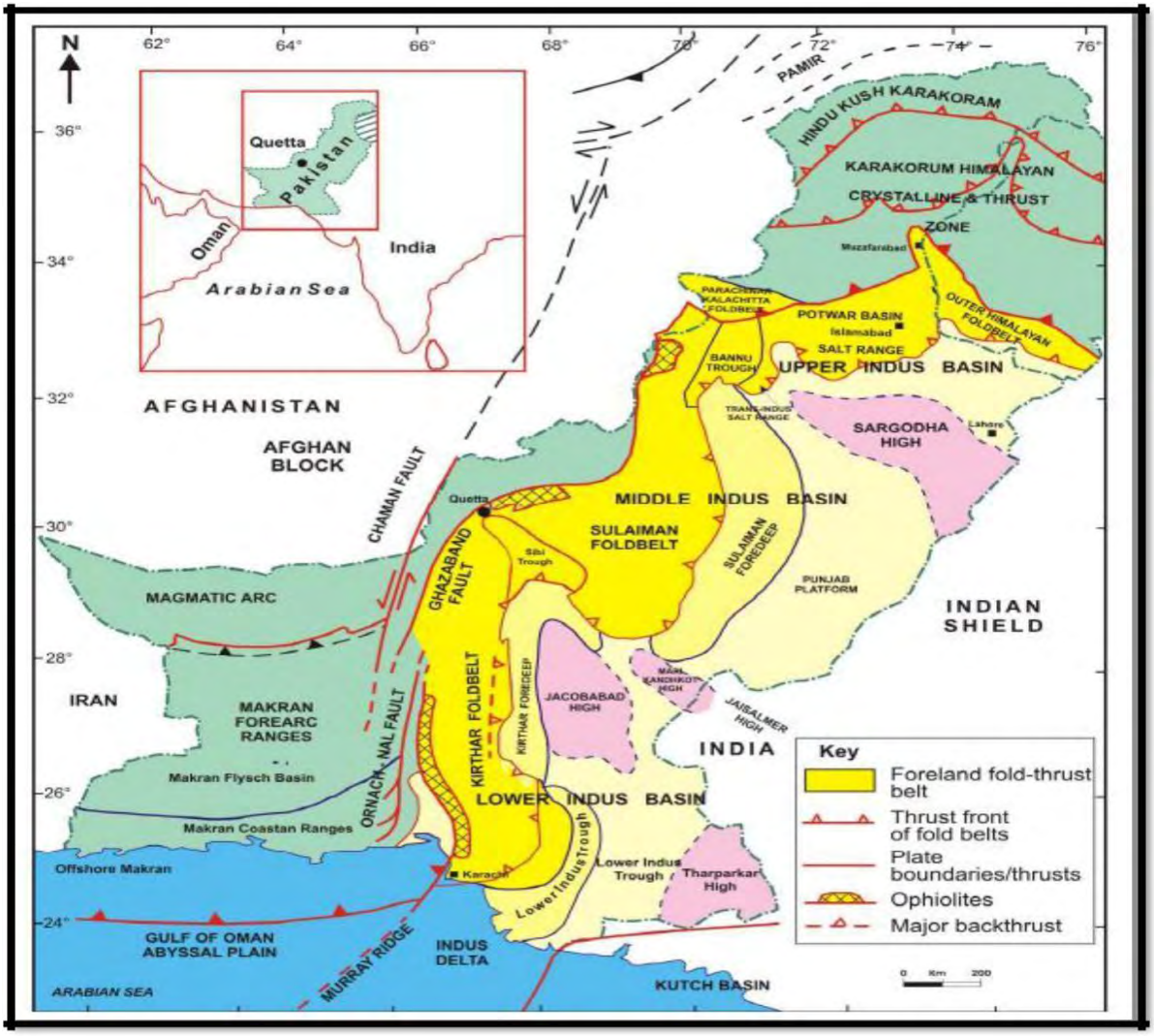

Figure (2.1). Location of Zamzama Block (Kadri, 1995)

2.4 Southern Indus Basin:

The Zamzama Block is located in the Kirthar Subbasin, which is part of the Southern Indus Basin. It is located to the south of the Sukkur Rift. The Southern and Central Indus Basins are separated by the Sukkur Rift. The Indian shield to the east and the marginal zone of the Indian plate to the west define the boundaries of the Southern Indus Basin. Its southern extension is bounded by the Murray offshore Ridge (Kadri, 1995). Southern Indus Basin consist of structure , which are

as follows:

1. Thar Platform
2. Karachi Trough
3. Kirthar Fold belt
4. Offshore Indus
5. Kirthar Foredeep

2.5 Kirthar Sub Basin:

Zamzama Block is located in the Kirthar Sub basin that is a part of the Southern Indus Basin and lies in the Kirthar Foldbelt. The Kirthar Subbasin is depicted in Figure 2.1, which depicts Pakistan's Basinal categorization as well as the subclassification of the Southern Indus Basin. The Indus Basin's Kirthar Fold Belt is a tectonic-stratigraphic province. The Kirther subbasin is part of the Indus extracontinental trough down warp basin, which formed on the Indian plate (Raza, 2002). The study area is the North-South extended tectonic feature known as the Kirther Fold Belt, which is structurally and stratigraphically comparable to the Sulaiman Fold Belt.

The Kirther Fold Belt is located along the western edge of the Indus Basin, which is connected to the Baluchistan Basin. The succession was deposited on the Indian Plate's northwestern passive border, which has been separated into the Sulaiman and Kirther blocks based on satellite pictures of its structural pattern (Raza, 2002).

The Kirthar Fold Belt was formed when the Indian Plate collided with the Eurasian Plate during the collision phase. It is made up of a continuous series of fold-thrust belts (Raza, 2002). The belt stretches 350 kilometres and is mainly north–south in direction (Kazmi and Jan, 1997). Late Pliocene–Pleistocene is considered to be the time of the largest mountain-building activity.

2.6 Petroleum History:

The first exploration well at Zamzama, Zamzama-1/ST1, was spudded in January 1998. Extended test wells (ETW) were drilled in 2001, and full production began in the middle of 2003. The well, which was drilled to a total depth of 3,938 meters, discovered hydrocarbons in the Khadro and Pab sandstones, and wireline logs verified a gas column of more than 300 meters. 3-D seismic acquisition and the drilling of the Zamzama-2 appraisal well were part of the appraisal program. The Zamzama-2 well was bored to a depth of 3,933 meters and found hydrocarbons in the Khadro

and Pab sandstone formations. Zamzama -03, 04, and 05 were also drilled as development wells. This field is an important source of gas, ranking fourth in the country in terms of gas output. With a low condensate to gas ratio of 6.5 barrels/MMcf, the gas is sweet and dry. The Zamzama gas field's anticipated production life is 15 to 25 years.

2.7 Structural Pattern:

Open and symmetrical folds dominate the Kirthar fold belt, which is generated by the inversion of basement-involved Jurassic extensional faults. Thrusts in the Eocene mudstones and thrusts with a deeper detachment in the Lower Cretaceous source rock period that involve the reservoir during deformation defined by horst and Graben structures, as well as a system of transcurrent faults, have been interpreted with two detachments. (Zaigham & Mallick, 2000). A considerable number of anticlinal structures were formed on the eastern side of the Kirther fold belt as a result of plate collision during the Oligocene–Miocene period (Zaigham & Mallick, 2000).

The research reveals Zamzama's structural style and evolution. Block that the predicted shortening along the Zamzama structure in figure (2.2) represents deformation similar to fault propagation folds. This indicates that a decollement exists beneath the structure, resulting in Zamzama being a thin-skinned structure with no basement involvement in the deformation.

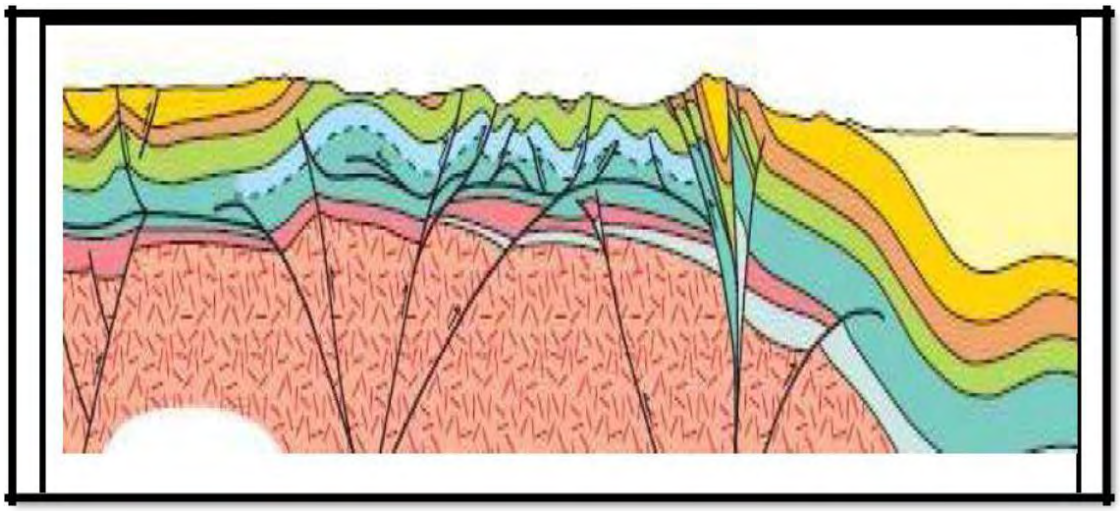

Figure (2.2). Structural pattern of Zamzama Block. (Abbasi et al,2016)

2.8 Stratigraphy:

The Kirthar Foldbelt Basin is projected to have a stratigraphic succession ranging from Permian to Recent, with substantial unconformities at the Permian, Jurassic, and Upper Cretaceous levels. The Cretaceous rocks in the Suleiman and Kirthar provinces of the Lower Indus Basin are largely sedimentary in origin and, except for small disconformities, form a continuous succession from Early to Late Cretaceous. In some portions of this area, the Tertiary layers are transitional, and local disconformities between the Cretaceous and Tertiary have been identified (Fatmi, 1972).

The Jurassic sequence is mostly limestone with some shale, whereas the Cretaceous sequence is made up of sandstone, shale, and limestone/marl. Overlain by the Paleocene Khadro, Ranikot, and Dunghan formations, the Cretaceous is unconformable. The Laki, Ghazij, and Kirthar Groups of the Eocene have limestone and shale lithology. Sandstone and shale make up the Oligocene to Pliocene Nari, Gaj, and Siwaliks sequence.

From the well tops, the following Zamzama Block groups and formations can be encountered. Figure (2.3) shows a stratigraphic map of the Zamzama block, which is detailed further below. The formation encountered in the Zamzama block is shown in Table (2.1)

Table (2.1). Formations List

1. Siwalik Group	9. Girdo Sandstone
2. Ranikot Group	10. Khadro Formation
3. Gaj Formation	11. Pab Sandstone
4. Nari Formation	12. Bhara Formation
5. Kirthar formation	13. Lakhra Formation
6. Ghazij Formation	14. Fort Munro Formation
7. Laki Formation	15. Parh Formation
8. Dunghan Formation	16. Kirthar Limestone

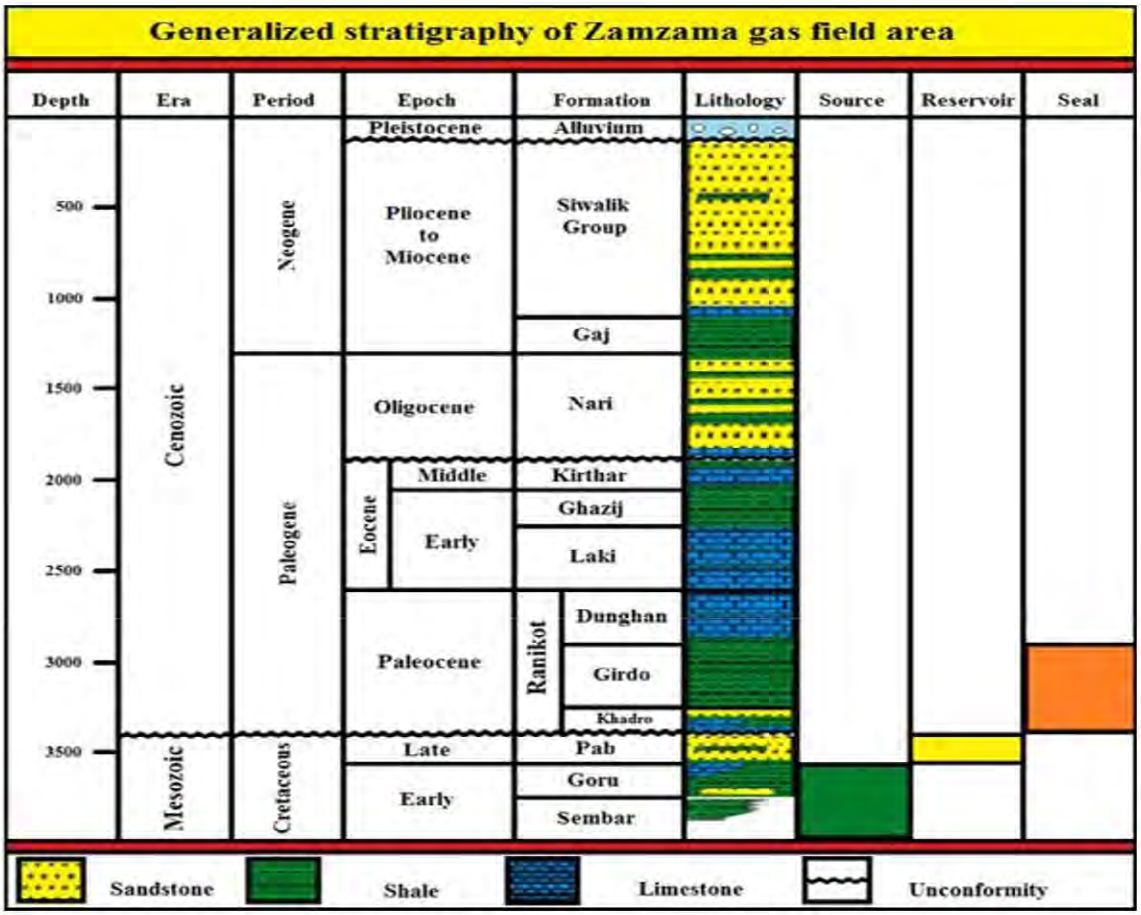

Figure 2.3 General stratigraphy of lower Indus basin (Abbasi et al., 2016)

Much of the Pab and Mughal Kot formations, which are widely exposed in western Pakistan, are made up of Late Cretaceous sandstones. These units, which are dominated by quartos sandstones with subordinate marls and argillites in the south-central part of the Kirther fold belt, were all deposited on the western continental border of the Indo- Pakistan plate (Asquith 2004).

2.9 Petroleum System:

With important fields including Zamzama Bhit, Mazarani, and Sari-Hundi, the Kirthar Foldbelt is a high-volume gas and gas condensate producer, confirming the presence of a dynamic petroleum system in this tectono-stratigraphic province. Except for the Bhit gas discovery, where gas is found in cretaceous layers, gas discoveries in the southern Indus basin are largely from paleocene deposits (Zaigham and Mallick 2000)

A mature source rock, a path to migrate hydrocarbons, reservoir rock, and the proper time for the

creation of these elements and the migration processes are all geological components and processes required to create and accumulate hydrocarbons.

2.10 Source Rock:

The Zamzama Field's source formations are the cretaceous Sember and Goru formation Shale. Goru shows a pelagic environment, whereas the sember was found on the shelf edge. The majority of the Sember deposits come from a marine environment. Sember's TOC ranges from 0.5 to 3.5 percent, with an average of 1.4 percent. Sembers with Type-III Kerogen, ranging from immature to adult (Badley, M. (1985)).

2.11 Reservoir Rock:

Reservoirs Rocks are porous and permeable rocks that have commercial hydrocarbon reserves. The most essential physical features of reservoir rocks for hydrocarbon accumulation are porosity and permeability. The reservoirs in the Kirthar Foldbelt are Jurassic to Eocene in age. The Foldbelt's principal objectives are Middle Jurassic carbonates, Lower and Upper Cretaceous sandstone, Paleocene sandstone and carbonates, and Eocene carbonates. The principal reservoir for the Zamzama field is the Cretaceous Pab Sandstone. It is found in a tidal and shallow marine environment. The Pab sandstone is a braid delta/coastal plain deposited formation with a lot of sand.

Limestone from the Habib Rahi and Pirkoh portions of the Kirthar Formation could be potential reservoirs in the Eocene. The Pab Sandstone, as well as the sand strata within the Mughal Kot Formation, is the research area's most promising reservoir. Throughout the Sulaiman and Kirthar Ranges, the Pab Sandstone has been shown to be a reliable reservoir. Potential reservoirs can be up to 400 meters thick. Sandstone porosities can reach 30 percent, although they're more typical in the 12 to 16 percent range, while limestone porosities range from 9 to 16 percent. These reservoirs have permeabilities ranging from 1 to > 2,000 milidarcies (md).

2.12 Cap Rocks:

The paleocene Khadro and Ranikot shale strata operate as a top seal for the underlying Pab sandstone (Badley, M. (1985)). These shales have proven to be reliable in bhit, zamzama, and Mehar fields, among other places. Khadro is sandy in some circumstances and does not act as an

effective seal, whereas Girdo formation does (Badley, M. (1985)).

2.13 Trapping Mechanism:

In the research area, a large N-S trending thrusted anticline acts as a trap (Jackson et al., 2007). On both sides of the fracture, gas was extracted. There is no vertical leakage, however there is cross-wall leakage (Badley, M. (1985)). In the zamzama location, the bounding fault does not reach the surface and acts as a seal component (Jackson et al., 2007).

CHAPTER#3
3D SEISMIC DATA INTERPRETATION:

3.1 Introduction:

The goal of interpreting 3D seismic reflection data is to find hydrocarbon accumulation beneath sedimentary rocks. Exploring hydrocarbons is a costly job. This risk exists because science has yet to uncover a direct technique of locating hydrocarbons or gaining access to large amounts of hydrocarbons in the subsurface. For proper interpretation, focusing entirely on seismic data is insufficient; knowledge of the location is also essential. Gravity and magnetic data, surface geology and topography, well log data, and physical and geological concepts are all included (Sheriff, 1999).

The essential abilities that are widely employed in the petroleum industry for exploration are seismic interpretation and subsurface mapping (Sen., 2006). Because of its high resolution, the seismic reflection method is one of the most essential indirect geophysical methods for petroleum exploration. In the early stages of petroleum exploration, other indirect methods such as gravity and magnetic are used. Seismic interpretation is the process of extracting subsurface information from seismic data collected on the earth's surface. It may also be used to determine the area's overall geological knowledge, as well as to locate projections for future exploratory well drilling or to manage the development of an already discovered field (Coffeen, 1986).

There are various phases required in interpreting 3D seismic data. These stages are performed to solve the seismic section in the context of all the recoverable stratigraphic and structural sequences. The primary goal of seismic analysis in the oil and gas industry is to find and discover the suitable location for trapped hydrocarbon in a given structure.

3.2 Techniques:

There are two techniques to analyzing seismic data, which are briefly mentioned below:

- Stratigraphic Analysis
- Structural Analysis

3.2.1 Stratigraphic Analysis:

The seismic section has a series of reflections that must be analyzed stratigraphically. The seismic expressions of genetically linked geological sequences are used to interpret seismic sections. Variation in a sedimentary deposition is how it is interpreted.

3.2.2 Structural Analysis:

The seismic section is related to structural analysis in order to identify prospective structures capable of holding and storing hydrocarbons. Instead of depth, two–way seismic reflection time is used in many structural interpretations. The main concern in this strategy for hydrocarbon accumulation is structural traps like anticlines, faults, and folds (Kearey, 1988).

3.3 Basic work flow of Seismic Interpretation:

The key interpretation steps used to understand 3D seismic data are as follows:

- Base map generation
- Synthetic Seismogram Generation
- Horizons and fault interpretation
- Time and Depth Contour Maps Preparation

Figure 3.1 demonstrates the seismic interpretation workflow.

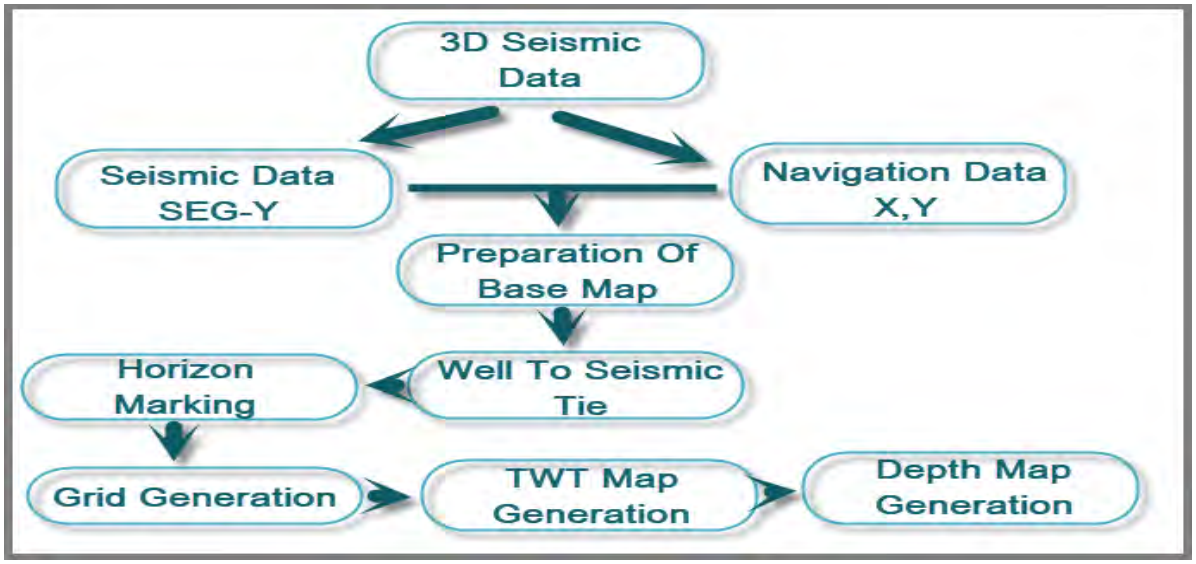

Figure 3.1: seismic interpretation workflow

3.4 Base map:

3D seismic data is represented as a cube with in-lines and cross-lines running along the x- and y-axes, respectively. Figure 3.2 shows a net geometry formed by in-lines increasing northward and cross-lines increasing eastward, both of which are orthogonal to each other.

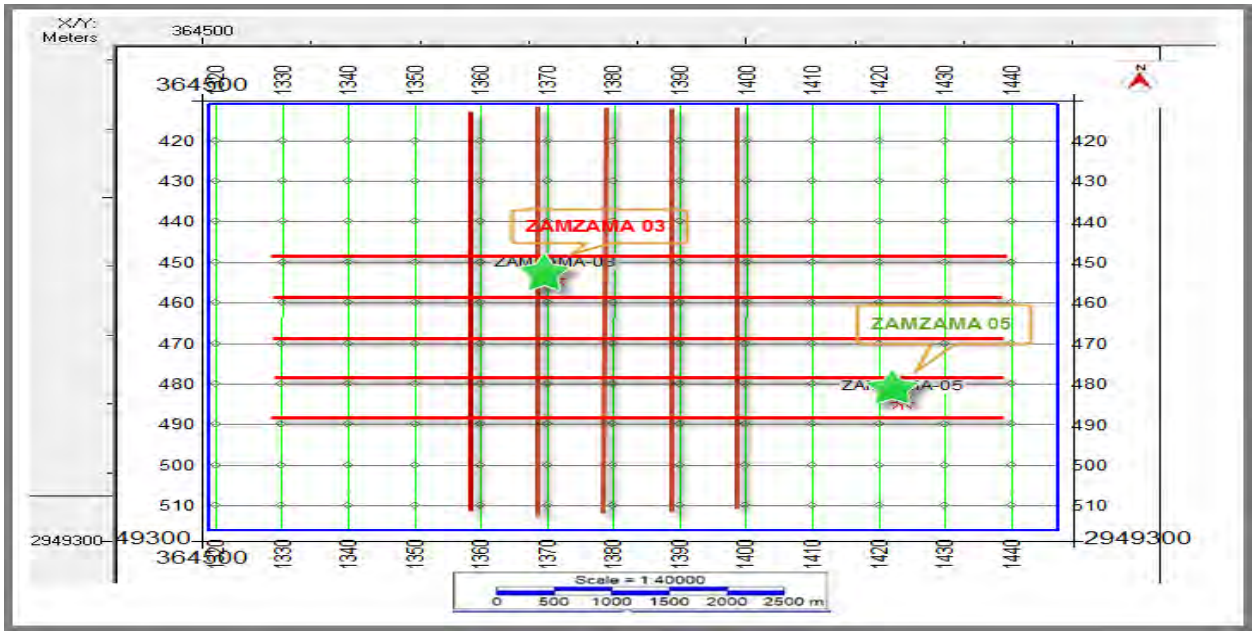

Figure 3.2: Basemap of study area

3.5 Generation of Synthetic Seismogram:

Based on the well logs (sonic and density) from well Zamzama – 03 It was created a synthetic seismogram. Figure 3.3 represents the synthetic seismogram generating workflow.

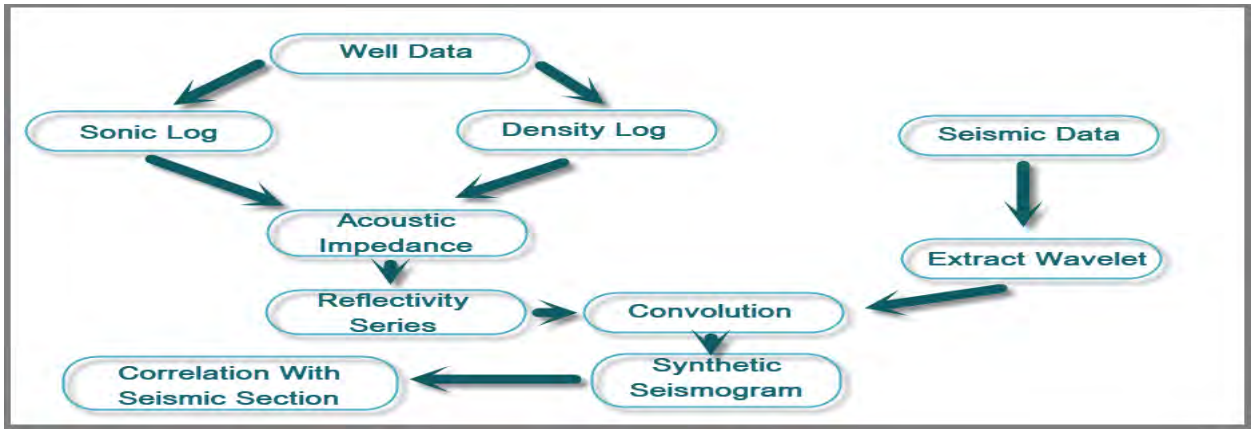

Figure 3.3: workflow of synthetic seismogram generation:

The horizon is confirmed using the generated seismogram. The following horizons have been taken:

- Khadro Formation
- Pab Sandstone (Sandstone, Late Cretaceous)
- Fort munro formation

Because in-lines lie on the dip of structures, they are chosen for interpretation. Three-dimensional data has two major faults in our case. Only two reverse faults are linked with the Hinge zone of the fold in the Zamzama gas field. Figure 3.4 displays a synthetic seismogram.

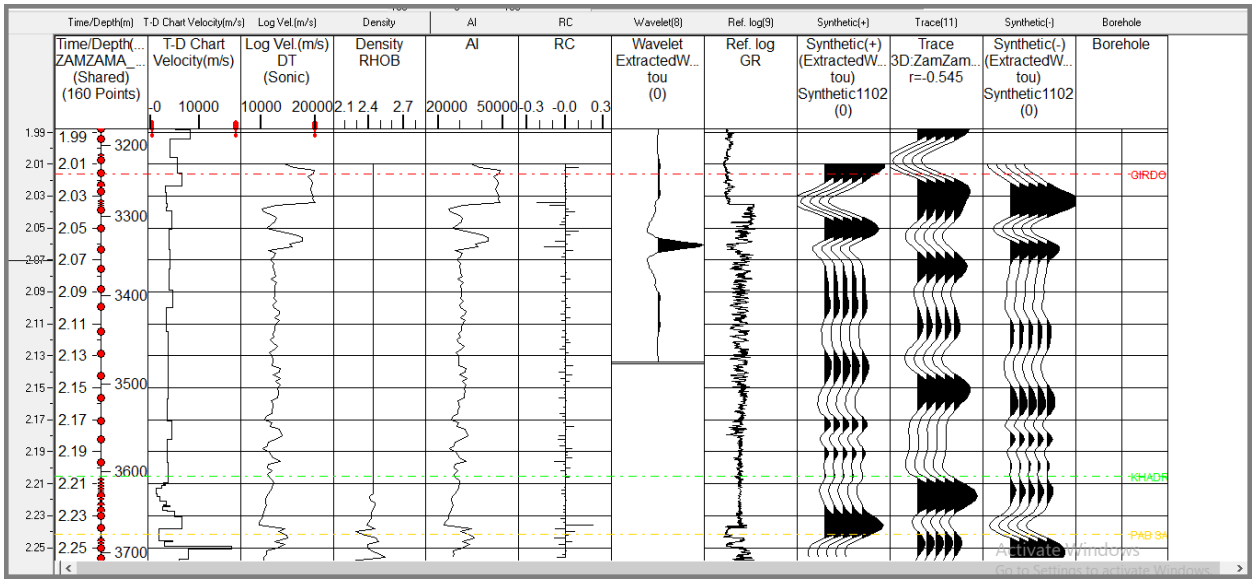

Figure 3.4: Synthetic seismogram for picking horizons on zamzama-03 well.

3.6 Interpretation of Horizons and fault :

The horizons are interpreted via Kingdom software; interpretation of horizons on seismic sections is the main responsibility of a seismic data interpreter, who should have a deep understanding of the area's structures and geology. Thus, understanding the relationship between geology and seismic section requires an understanding of the significance of lithological change (Badly, 1985).

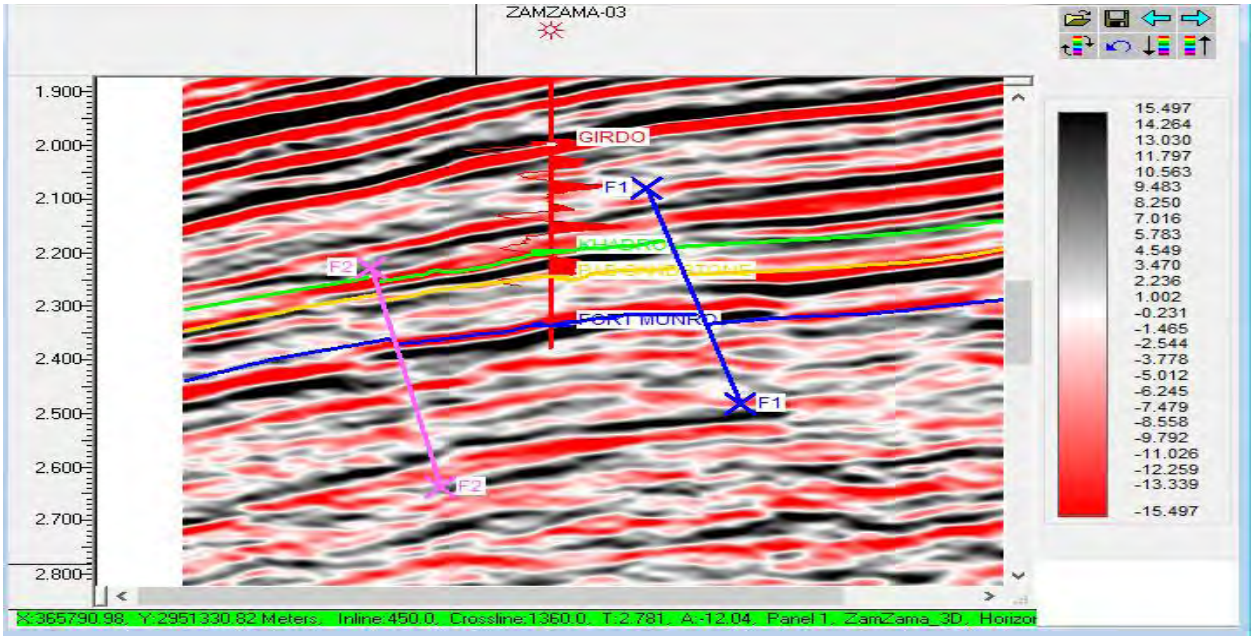

Figure 3.5: Interpreted seismic inline 450 and crossline 1360 having faults F1 and F2 and three horizons Khadro , Pab and Fort munro.

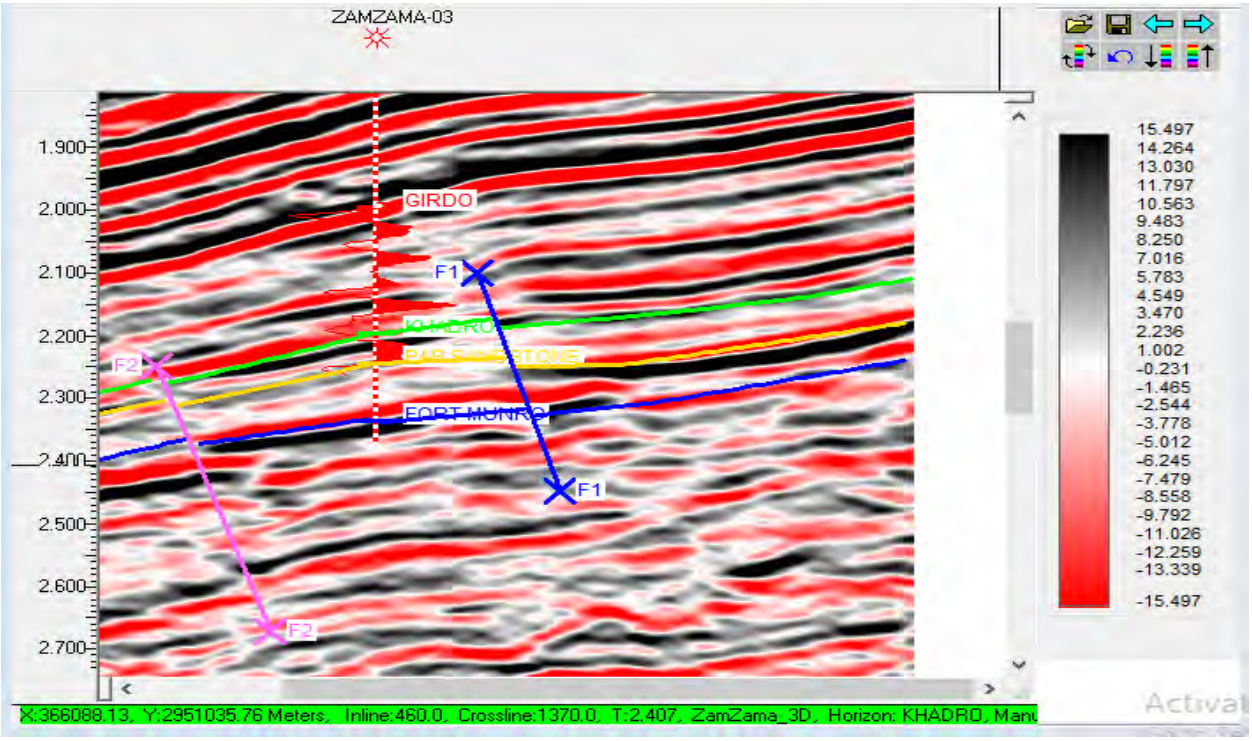

Figure 3.6: Interpreted seismic inline 460 AND crossLine 1370 having faults F1 and F2 and three horizons Khadro , Pab and Fort munro.

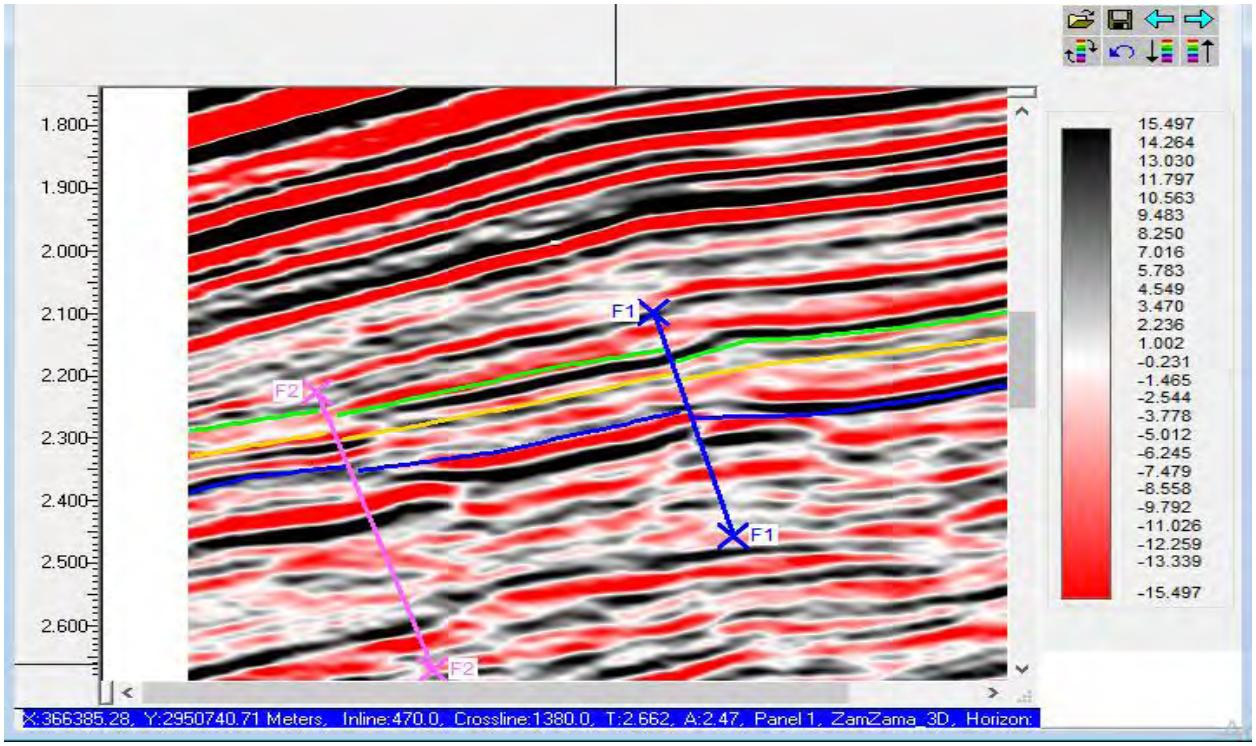

Figure 3.7: Interpreted seismic inline 470 AND crossLine 1380 having faults F1 and F2 and three horizons Khadro , Pab and Fort munro.

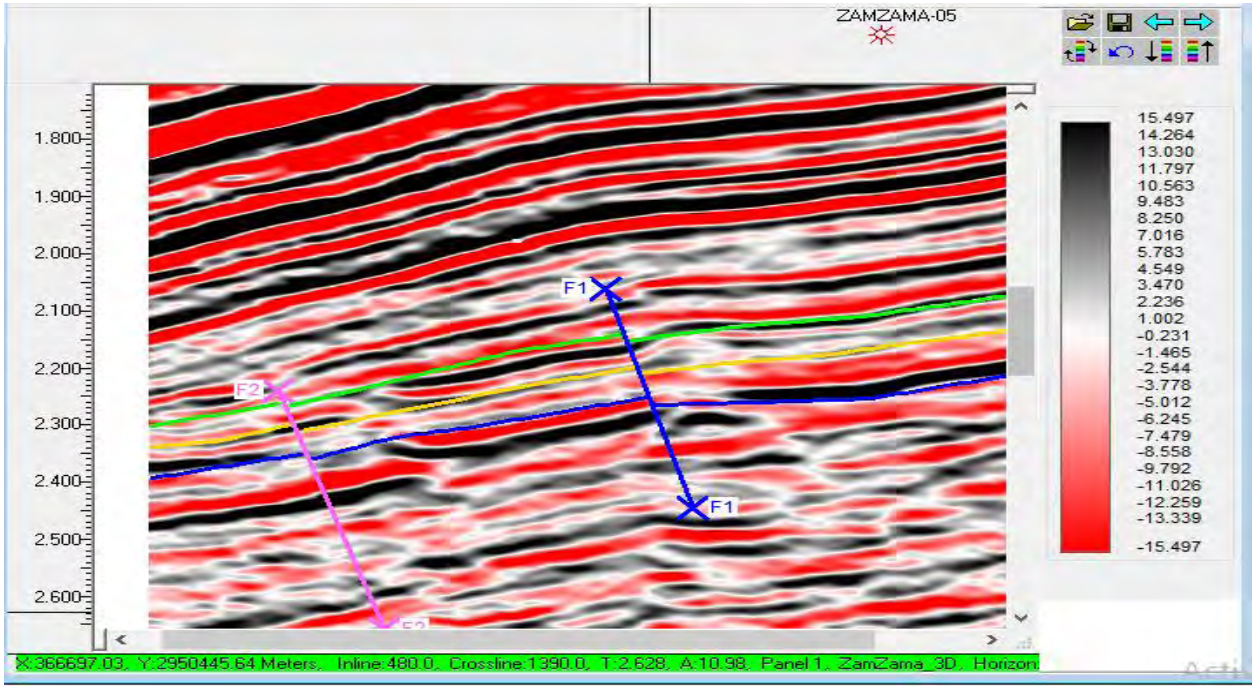

Figure 3.8: Interpreted seismic inline 480 AND crossLine 1390 having faults F1 and F2 and three horizons Khadro , Pab and Fort munro.

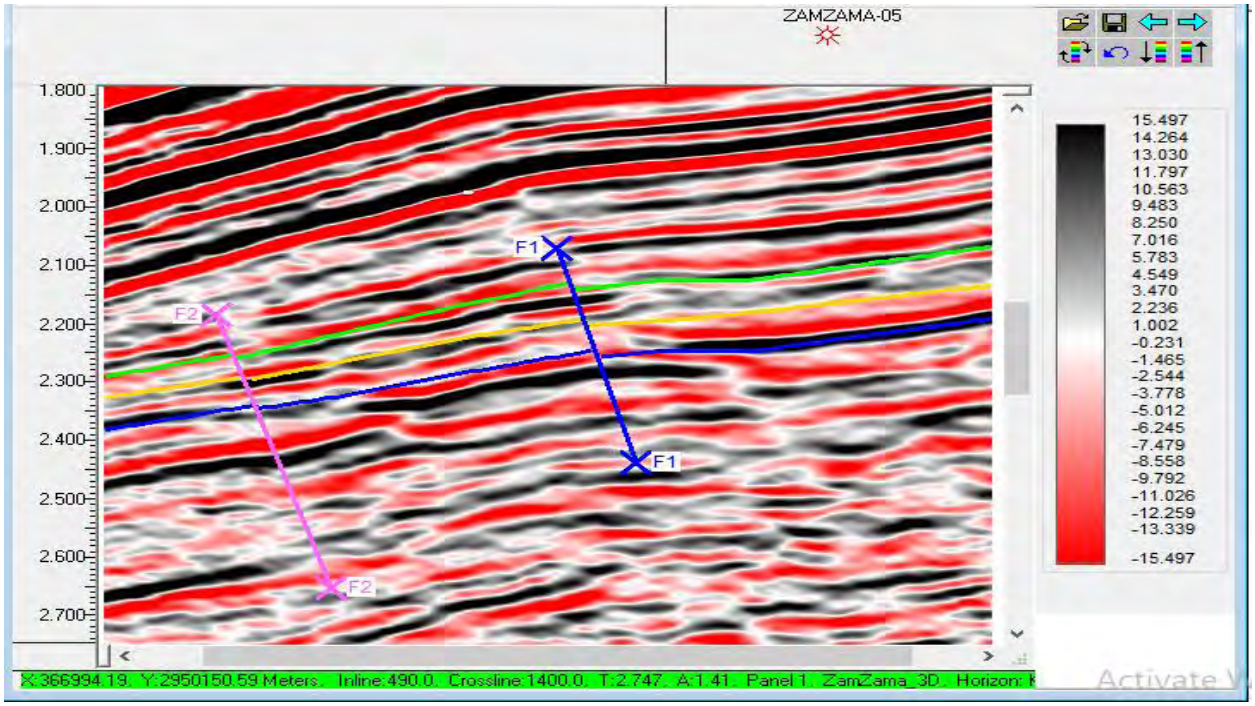

Figure 3.9: Interpreted seismic inline 490 AND crossLine 1400 having faults F1 and F2 and three horizons Khadro , Pab and Fort munro.

To highlight the exact location of the horizons on the seismic section, the well tops are correlated with the seismic. Three horizons were interpreted on seismic section based on Zamzama – 03 well tops. Figure 3.5 , 3.6 , 3.7 , 3.8 and 3.9 indicate three horizons, the Khadro , Pab and Fort munro.

Faults are marked by amplitude decay, reflector discontinuity, distortion, or absence of the reflection. Only two faults, F1 and F2, are marked here, both of which are thrust faults.

Horizons are important to mark because we need to grid and contour our structure, therefore we can use the synthetic seismogram we previously developed to indicate different horizons. Based on the information available, the khadro, Pab and fort munro formations were selected.

3.7 Fault polygon construction:

To create the fault polygon shown in Figure 3.10, we must select faults on seismic sections at particular intervals, connect them, and cover the area in between for the grids to recognize it as a faulted area. If we don't transform them into fault polygons, the software won't recognize them as a discontinuity, giving us an inaccurate representation of the area.

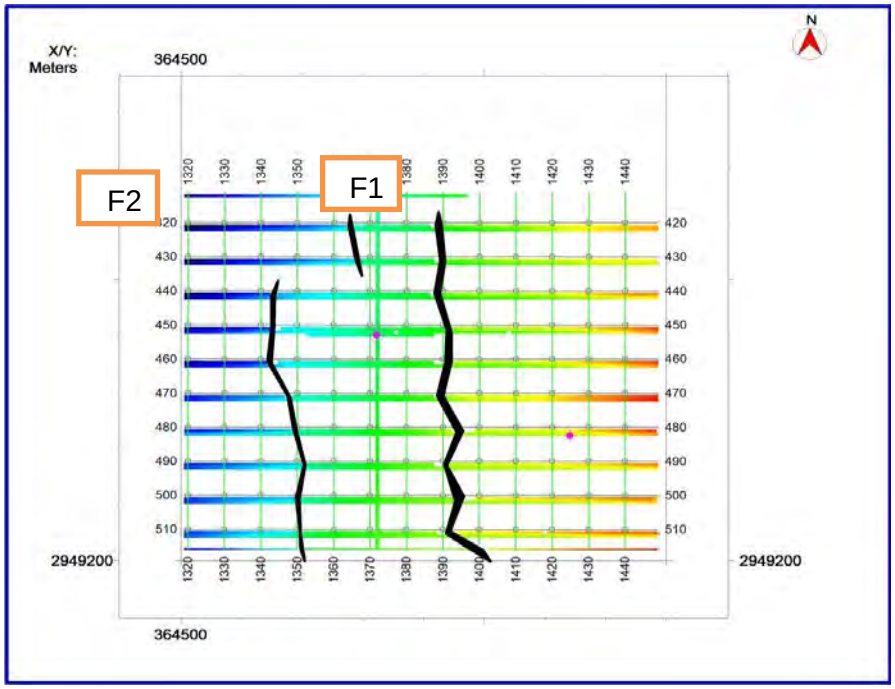

Figure 3.10: Fault Polygon of Faults F1 and F2 along Pab Formation.

3.8 Contour Maps:

The contour maps, time or depth, are the end products of all seismic exploration. The mapping is one of the most crucial aspects of data interpretation, on which the entire operation is based. Contours are lines that connect points with similar values (Coffeen, 1986). Contours are used to translate a three-dimensional earth surface into a two-dimensional one. These contour maps show the formation's structural relief, as well as any faulting and folding, as well as strata dip.

3.8.1 Preparation of Time and Depth Contour maps:

The generation of depth and time contour maps is the next procedure in seismic interpretation. Time contour maps were created first because seismic data is in the time domain, and then depth contour maps were created by transforming seismic data from the time domain to the depth domain using velocity models. Contour lines are defined as lines of similar depth or time moving across a map as expressed by data (Coffeen, 1986).

The weighted average algorithm is used to create the time contour maps. This is the best algorithm for places with a lot of complexity, such as Zamzama. The time model's contour interval is 0.008 seconds.

Using the true velocity from wells available in the research area, both time contours were transformed into depth contour maps using the formula in equation 3.1.

$$s = v * t/2 \quad (3.1)$$

Using KB as a reference datum, depth contour maps were created, and time contour maps were created using the weighted average algorithm. The depth model contour interval is 12.5 meters.

The structural relief, formation slope, dip, and any folding and faulting are all visible on these contour maps. These time and depth contour maps were created using Seismic Micro Technology HIS (Kingdom 8.8).

The time contour maps of the khadro formation, Pab sandstone and fort munro formation were created by marking the two-way time of these formations on seismic sections and contouring it. On the seismic section, the two-way time contour and its trend show that a flank or limb of an anticline structure is present in the Zamzama area.

3.9 Pab Sandstone:

The time and depth contour maps of Pab sandstone are shown in Figures 3.11 and 3.12. The light yellow color represents the lowest time, while the blue color represents the highest time, indicating the deepest regions of an anticlinal structure's flank or limb. The light yellow color on the depth contour map shows the lowest depth, while the blue color denotes the highest depth. The dipping limb of an anticline from north to west could be seen on the time and depth contour maps. Pab sandstone is a flank or limb of an anticline-like formation, as shown by color contrast and contour trends.

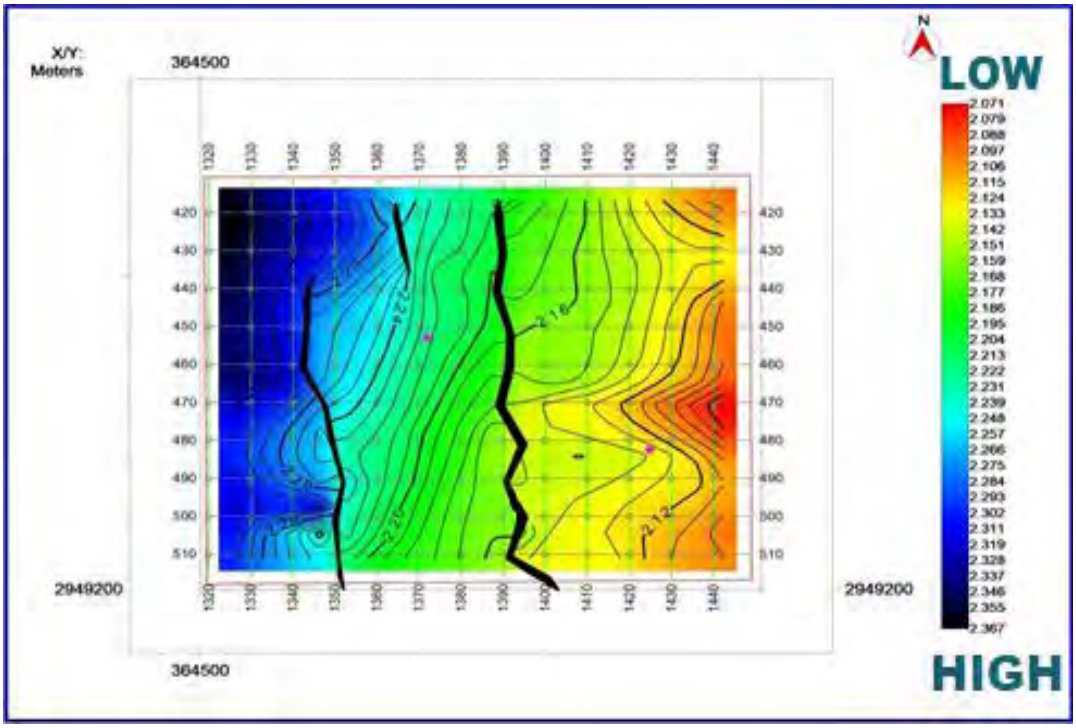

Figure 3.11: Time contour map of Pab Sandstone.

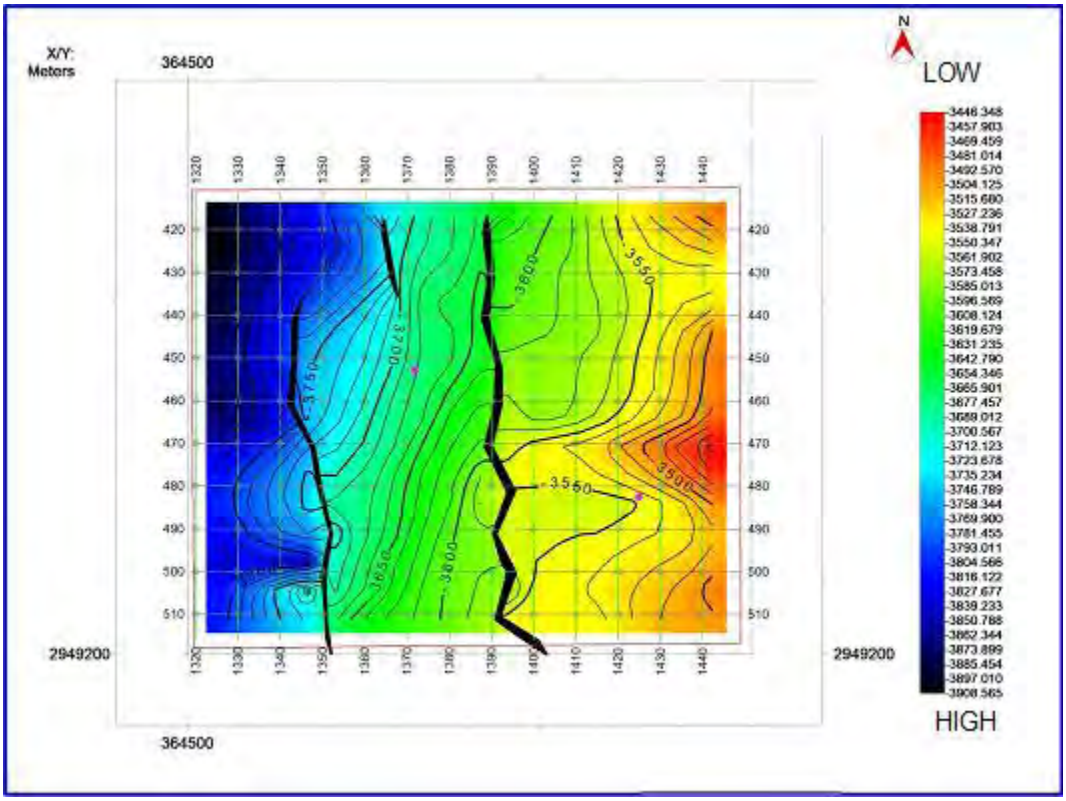

Figure 3.12: Depth contour map of Pab Sandstone.

CHAPTER#04
PETROPHYSICAL ANALYSIS

4.1 Introduction:

The study of the physical qualities of rocks that are connected to incidences, rock body behavior, and fluid inside the rocks is known as petrophysical analysis. Reservoir representation is a critical stage in the petroleum industry since it helps in the definition and identification of well and field potential, as well as the identification of reservoir zones that contain hydrocarbons and can be recovered (Cosgrove et al., 1998).

Petrophysics is a process for estimating and representing reservoir properties. Petrophysics research helps in the detection and quantification of fluids in reservoirs (Rider, 1995). The interpretation of well logs is referred to as petrophysics. Well logging is the process of taking precise measurements of geological and geophysical factors when a well is drilled down. The "Sonde" is a well logging equipment that examines the physical and chemical properties of the rocks as well as their interaction with fluids (Rider, 1995).

Porosity, shale volume, hydrocarbon saturation, and water saturation are essential reservoir physical parameters to characterize precisely the probable hydrocarbon-bearing zones. Geophysicists and geologists can use a combination of petrophysics and rock physics to assess risk and opportunities in a given location. Well, measurements are used in petrophysical analysis to help reservoir description (Daniel, 2003).

4.2 Data Loading:

Spontaneous Potential (SP) log, Caliper log, Sonic log (DT), Gamma Ray log (GR), Density log (RHOB), Resistivity log, Neutron log, Latero log shallow (LLS), and Latero log deep (LLD) were some of the logs available (LLD). These logs are organized into three different tracks: lithology, porosity, and resistivity. Gamma ray log, Caliper log, and SP log are all part of the lithology track. Based on these log curves, the parameters for petrophysical analysis are established as follows:

- Volume of shale
- Water saturation
- Hydrocarbon saturation

These logs are expressed in depth vs. linear scale. Caliper logs range in thickness from 4 to 16 inches and are used to calculate well thickness. The SP log was used to display the structure in mV as it progressed in depth. The GR log is used to determine the amount of radiation in the well. API is used to express these parameters. The LLD and LLS resistivity tracks are measured on a logarithmic scale from 1.00 to 1000 ohm. There are three types of porosity tracks: neutron log, density log, and sonic log. These logs are used to calculate the porosity of a formation.

4.3 Work Flow:

A petrophysical analysis is used to examine the reservoir of well Zamzama-03 in the Dadu area of the lower Indus basin. The petrophysical analysis workflow chart is presented in Figure 4.1 below.

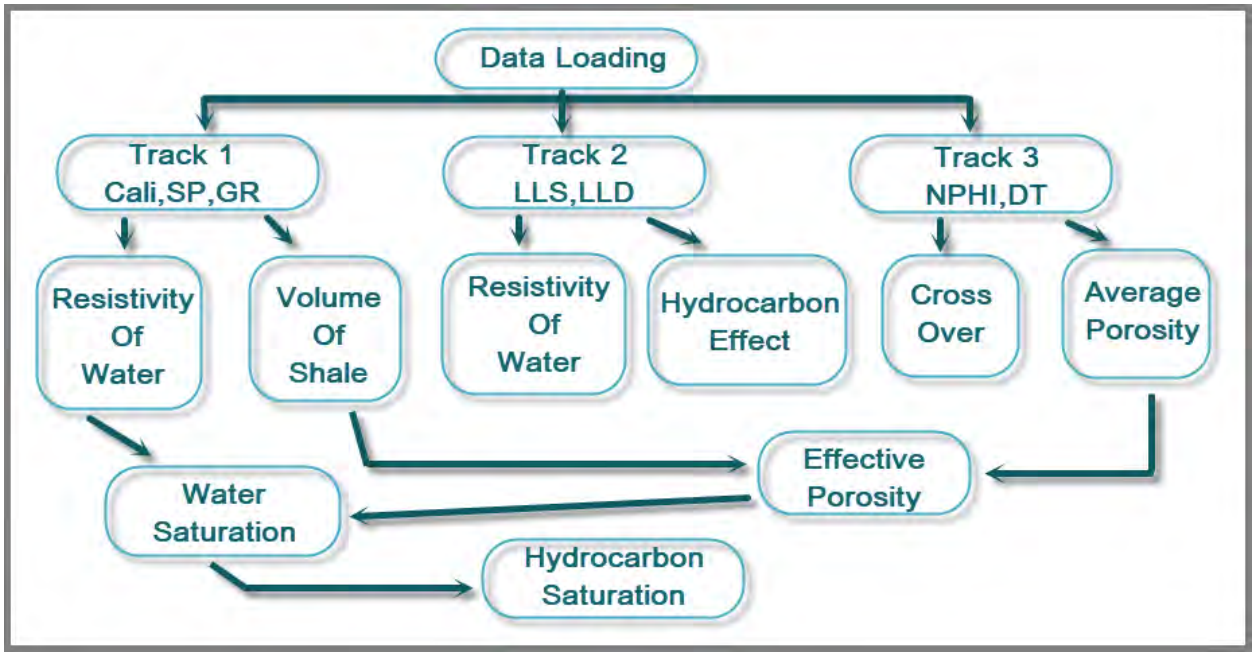

Figure 4.1: Show the workflow of petrophysical interpretation.

4.4 Volume of Shale:

The GR log is most commonly used to calculate shale volume. To calculate the volume of shale, it is assumed that radioactive materials are only present in shale and not in sand, which is known as clean sand.

The electromagnetic particles emitted from the formation are measured by the GR log. Photons are the name for these particles. The GR log is used to visualize and count these particles on a per-

second basis. The GR log is mostly used to distinguish between sand and shale (Daniel, 2003).

The amount of shale in the formation can be calculated using the formula below (Asquith and Gibson, 2004). In Equation 4.1, the volume of the shale equation is shown.

$$V_{sh} = \frac{GR_{log} - GR_{min}}{GR_{max} - GR_{min}} \quad (4.1)$$

where

V_{sh} is the volume of shale

GR_{log} show the reading on GR log at that point

GR_{min} is the minimum value of the GR log, and

GR_{max} show the maximum value of GR log

4.5 Porosity calculation:

The porosity of a formation will be determined by dividing the volume of the pores by the overall volume of the formation.

The porosity of a rock formation is calculated using neutron, density, and sonic logs.

Porosity from Sonic log:

The transmitter and receiver that transmit and receive sound waves make up a device that records sound waves. The instrument is used to measure the time it takes for a wave to go through one foot of formation to record the transient time. The duration of the transient interval is determined by the porosity and lithology of the rock formation (Daniel, 2003).

The following formula, presented in equation 4.2, is used to calculate the porosity of rock based on a sonic log .

$$\emptyset_s = \frac{DT_{log} - DT_{matrix}}{DT_{fluid} - DT_{matrix}} \quad (4.2)$$

where

$\emptyset_s$ is the porosity from sonic log.

DT_{log} is transient time of rock formation,

DT_{matrix} is transient time of the formation matrix,

DT_{fluid} is transient time of the formation fluids.

4.5.1 Porosity from Density log:

Because the porosity and rock type affect the density of a rock, the porosity may be estimated by knowing the rock type (Asquith and Gibson, 2004). The bulk density is recorded by the density logs, which combine the density of the grain and the fluid in the formation. Equation 4.3 shows the formula used to compute the formation's density porosity (Asquith and Gibson, 2004).

$$\emptyset_d = \frac{\rho_{matrix} - \rho_{log}}{\rho_{matrix} - \rho_{fluid}}, \quad (4.3)$$

where

$\emptyset_d$ is the density porosity,

ρ_{matrix} is density of matrix,

ρ_{log} is the bulk density of formation,

4.5.2 Porosity from Neutron log:

The concentration of hydrogen ions in the rock formation is measured by the neutron log. In this process, neutrons are emitted by lowering a sonde into a borehole, and these neutrons collide with nuclei of hydrogen atoms present in the fluids within the pores of the formation, losing some of their energy. This energy loss is linked to formation porosity (Asquith and Gibson, 2004). When clean sand is filled with water or hydrocarbon, the neutron log quantifies the liquid-filled porosity. The concentration of hydrogen in gas molecules is lower than in oil molecules, resulting in a very low porosity value. The presence of gas in a deposit causes a low neutron porosity value, which is referred to as the gas porosity effect (Asquith and Gibson, 2004).

4.6 Average Porosity:

Because individual logs have varying porosities, dividing all porosities by the total number of logs

gives the average total porosity. The relationship indicated in equation 4.4 is used to compute the total average porosity of Pab sandstone.

$$\emptyset_{avg} = \frac{\emptyset_n + \emptyset_d + \emptyset_s}{3}, \quad (4.4)$$

where

$\emptyset_{avg}$ is the average porosity of well,

$\emptyset_n$ is neutron porosity,

$\emptyset_d$ is density porosity,

$\emptyset_s$ is sonic log porosity.

4.7 Effective Porosity:

By removing the effect of shale in that rock, effective porosity is defined as "the ratio of the total volume of rock body to total volume of interconnected pores spaces that are present in the rock unit." The Effective porosity is used to calculate hydrocarbon and water saturation. The formula in equation 4.5 is used to calculate effective porosity (Asquith and Gibson, 2004).

$$\emptyset_{eff} = \emptyset_{avg} \times (1 - V_{sh}), \quad (4.5)$$

where

$\emptyset_{eff}$ represent effective porosity,

$\emptyset_{avg}$ is average porosity,

V_{sh} is volume of shale.

4.8 Resistivity of Water:

Different approaches can be used to calculate the water resistivity. The resistivity of fluids and formation resistivity can be calculated using two different tests. The first test is a direct measurement, in which an electric current is passed between two electrodes on logging equipment, followed by a potential drop, which gives us the resistivity. In the second test, which is an indirect measurement, the conductivity is measured by producing a current in the formation in the

borehole, and it can detect the current. The resistivity can then be estimated by taking its inverse (Krygowski, 2003).

To compute the resistivity of water, first, determine the Rmeq using Figure 4.2, and then use Figure 4.3 to calculate the resistivity of water.

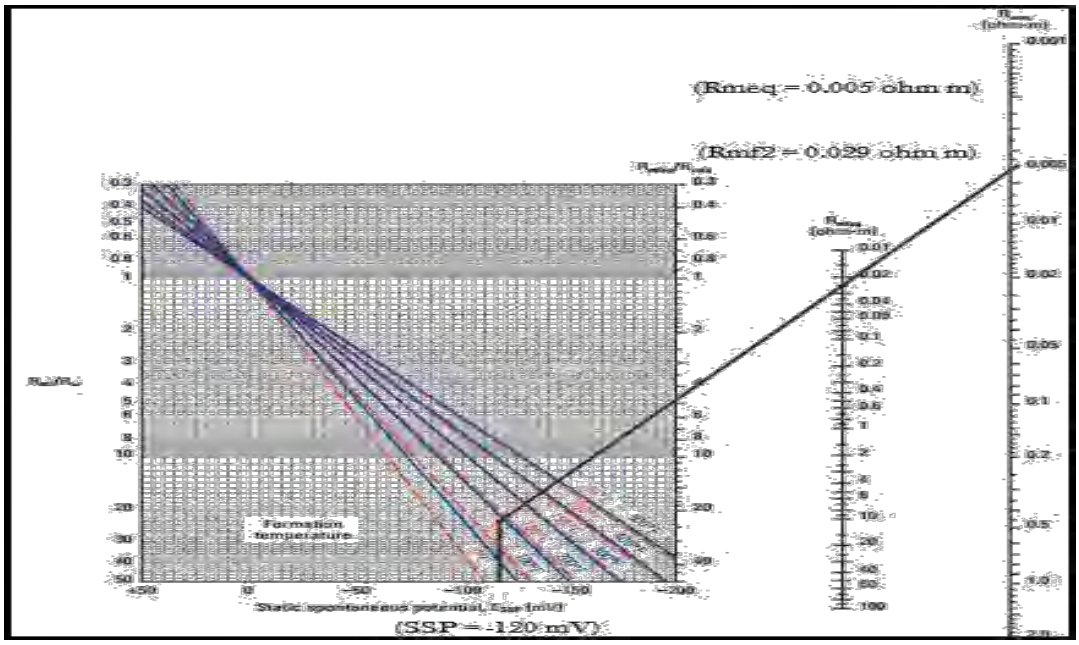

Figure 4.2: Determination of Rmeq from SP chart (Schlumberger, 1989)

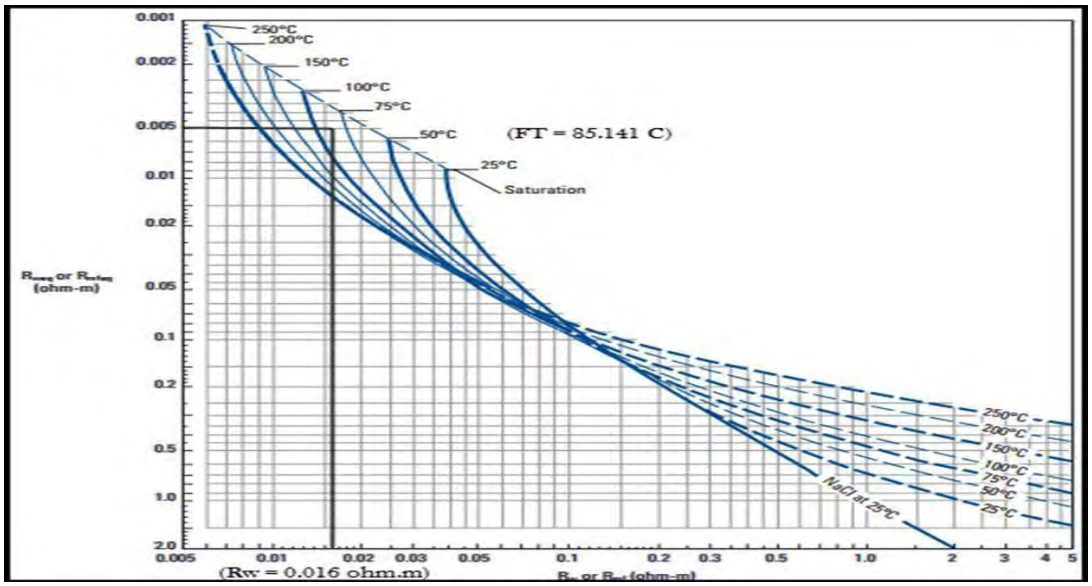

Figure 4.3: Determination of Rw from SP chart (Schlumberger, 1989)

4.9 Water Saturation:

Water saturation refers to the volume of voids in formation rock that are filled with water. Archie's equation, shown in equation 4.6, is used to compute the formation's water saturation by using equation 4.7.

$$S_w = \sqrt[n]{\frac{F \times R_w}{R_t}}, \tag{4.6}$$

where

S_w is the water saturation,

R_w is the resistivity of water in the formation,

R_t is actual resistivity,

n is the saturation exponent.

In the above equation F is known as the formation factor and is given in equation 4.7;

$$F = \frac{a}{\emptyset^m}, \tag{4.7}$$

where

a is constant,

$\emptyset$ is effective porosity,

m is the cementation factor.

4.10 Well Log Interpretation of Zamzama – 03:

The HIS Kingdom software is used to do the petrophysical interpretation of well Zamzama – 03 in order to identify the hydrocarbon zones. The petrophysical examination of the well is completed using several log curves.

The GR log is a good first indicator for lithology since it indicates where shale can be found. The percentage of shale will be higher if the GR values are higher. As a result, we can easily identify the clean zone or shale-free zone using this log. The well log interpretation for Zamzama - 03 is given in Figure 4.4.

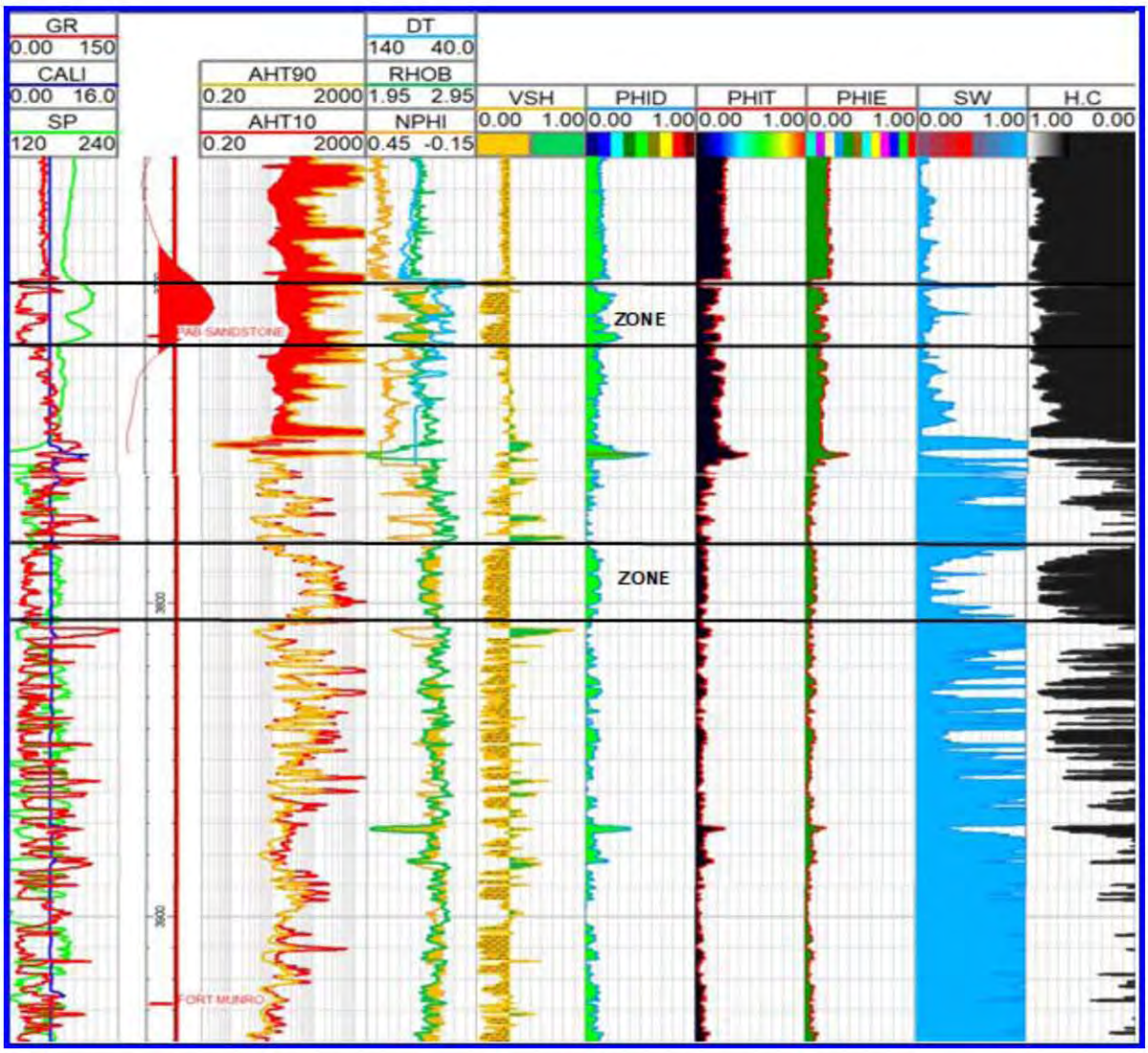

Figure 4.4: Shows the well log interpretation of Zamzama – 03

Similarly the extracted reservoirs parameter is given as below table 4.1 .

Table 4.1: Calculated values of Pab formation at Zamama 03 well.

	Zone A	Zone B
Gross Thickness	3702-3720 (18 m)	3783-3805 (22 m)
Volume Of Shale	10%	9%
Effective Porosity	15%	10%
Water Saturation	12%	31%
Hydrocarbon Saturation	88%	69%

Clean lithology has a low value in the GR log. The calliper log is straight, indicating that there is no disturbance within the borehole. We have separation in the resistivity logs LLD and LLS, as well as the crossover between the density and neutron logs. We have low water and high hydrocarbon saturation, therefore effective porosity is also quite good and meets the requirements for a reservoir. We marked the area into two zones based on these findings.

4.11 Hydrocarbon Saturation:

Hydrocarbon saturation refers to the presence of hydrocarbons in the pore spaces of a rock formation. "Sh" stands for hydrocarbon saturation (Kamel and Mabrouk, 2002). The formula provided in equation 4.8 could be used to determine the amount of hydrocarbon in the void spaces.

$$Sh = 1 - Sw\ , \qquad (4.8)$$

where

Sh is the saturation of hydrocarbon,

Sw is the saturation of water,

This is an indirect method for determining the remaining hydrocarbon content in voids.

4.12 Facies Analysis:

From the log data of the Zamzama well 03., we construct cross plots of Sonic log (DT) versus Neutron porosity log (NPHI) for the facies analysis of the Pab formation. These cross plots helped us in identifying the major lithologies present in our Pab formation reservoir.

4.12.1 DT vs NPHI Crossplot:

Using log data, a crossplot between DT and NPHI is created, with the Gamma ray log as a reference on the Z axis. The main reservoir is located between the depths of (3699-3748 m).

As shown in Figure 4.5, the DT log is associated with lower values of the gamma ray logs, indicating a clean formation, i.e. Sand. We have low DT values due to compact sand. In Sand, the NPHI log shows the same trend. We label it as sand in the red polygon, shaly sand in yellow, and shale in green.

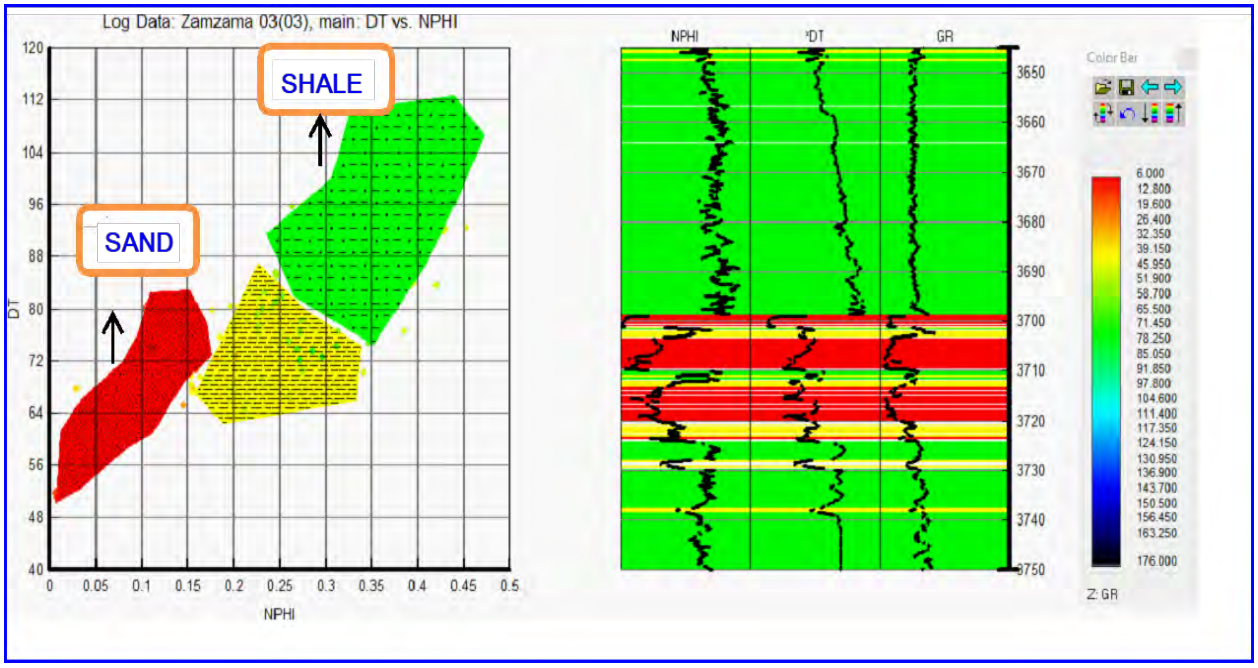

Figure 4.5: Lithology identification between sand and shale through crossplot between DT vs NPHI.

Only sand particles are found in our reservoir, hence the cluster of dots indicates pure lithology of sand. As a result, we concluded that the reservoir is primarily made up of Sand. While the high DT and gamma-ray values represent shale and we also have interbedded shale. The fact that DT log values increased in the second polygon, which we have classified as shaly sand, more increase in value indicates shale.

CHAPTER#05

Post Stack Inversion Analysis

5.1 Introduction:

We can use geophysical inversion to recover the subsurface spreading of physical attributes from data gathered in the field. One or more inversion algorithms can be used to invert each type of geophysical data . In recent years, the study of inversion in conjunction with seismic research has grown in popularity. Because of its increased strength and simpler assumptions, seismic post-stack inversion is the most preferred method. Broadband and band-limited inversion are the two methods for post-stack inversion, respectively (Russell et al., 2006). Model-Based and Sparse Spike Inversion are two types of broadband inversion.

From seismic and well log data, attributes of post-stack seismic inversion are now commonly utilized to estimate density, impedance, and Vp/Vs, as well as the elastic impedance. The exploration industry may easily implement the inversion approach because of its efficiency and increased quality for extracting rock physical attributes from seismic data . Inversion procedures begin with the creation of an initial geological model and use a trial-and-error method to match it to real seismic data. The model's parameters are updated until the generated data matches the seismic data. For estimating the distribution of physical attributes of the reservoir, a final fitted geological model is employed (Veeken & Da Silva, 2004).

The seismic data from the Zamzama gas field is subjected to Model-Based Inversion (MBI). Density volumes and P-impedance are reversed from the data. A high-resolution image is shown in the final stacked portion. The inversion reveals low impedances within particular hydrocarbon sand. The presence of a reservoir zone is unambiguously confirmed by the results of post-stack inversion. MBI approaches have the lowest error and a greater correlation coefficient than other methods. Even where well data is missing, the geostatistical technique populates the Petrophysical parameters (porosity, fluid saturation, shale volume, etc.) over the full seismic section. Geostatistical approaches are used to estimate the surfaces of known data points, and the points that lie between these surfaces are interpolated and filled with appropriate values (Haas and Dubrule, 1994).The seismic post-stack workflow is shown in Figure 5.1 .

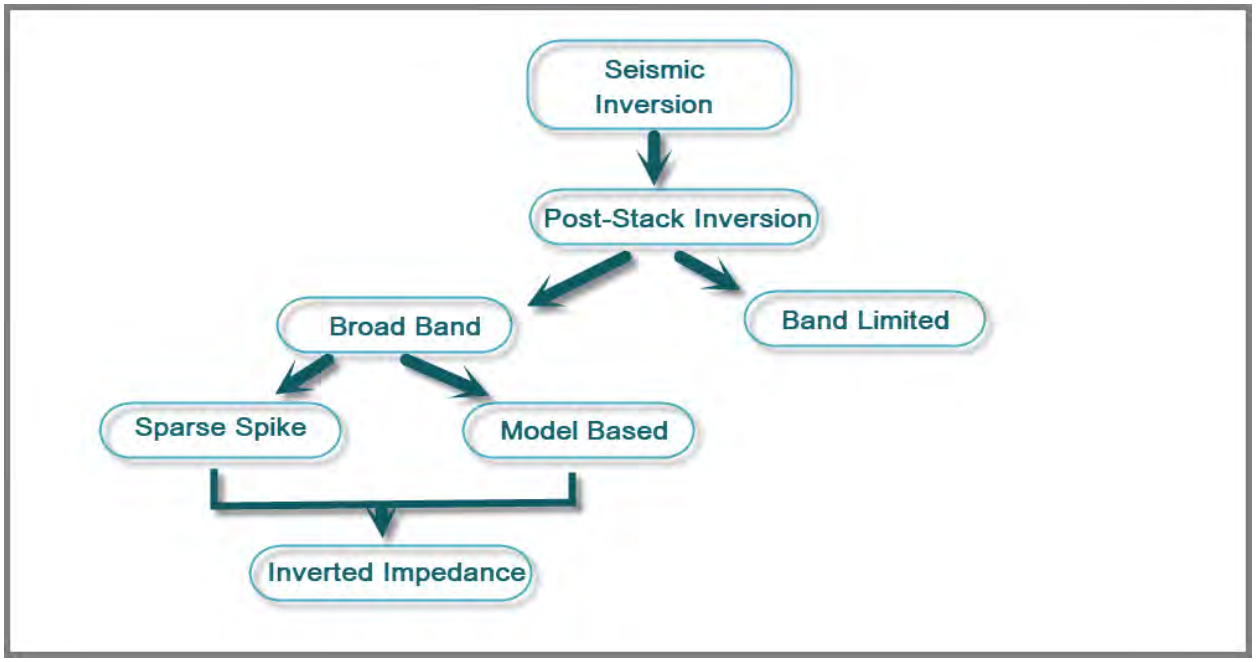

Figure 5.1: Workflow adopted for seismic post-stack inversion.

5.2 Methodology

Seismic inversion is based on convolution model. It is a convolution of earth reflectivity Rt , with the wavelet Wt and the addition of noise Nt where, $\otimes$ is the convolution operator.

$$S_t = R_t \otimes W_t + N_t ,$$

Where, St is the seismic trace, Rt is earth reflectivity, Wt is wavelet, Nt is noise. Assume noise component is negligible, so above equation becomes,

$$S_t = R_t \otimes W_t$$

Normal incidence earth reflectivity Rt is calculated by equation:

$$Rt = \frac{\rho j+1\, Vj+1 - \rho j Vj}{\rho j+1\, Vj+1 + \rho j Vj} ,$$

where, $Z_t=\rho_j V_j$ is impedance, V_j is compression wave velocity, ρj is the density and layer j overlie on layer j+1.

Inversion is process of estimation of inverse wavelet, convolving inverse wavelet with seismic data to get reflection coefficient, by rearranging above equation impedance of each layer calculated by equation (Russell, 2006).

$$\rho_{j+1}V_{j+1} = \rho_j V_j \frac{1+R_j}{1-R_j}$$

Above equation transform interface reflection coefficient to layer properties.

5.3 Extracted Statistical Wavelet

It's not straightforward to combine wavelet and reflectivity to create a synthetic trace. The shape of a seismic wavelet changes over time and is quite complex. The various inversion methods necessitate increasingly precise wavelet estimating methods (Russell et al., 2006). Wavelets vary depending on the subsurface location, and they are not all the same. Wavelet has a lot of problems because of issues like geometrical spreading and subsurface attenuation (Barclay et al., 2007). This research makes use of a statistical wavelet. The statistical wavelet extraction time frame is from 2150 to 2400 m, with a wavelength of 200 m and a taper length of 25 m. Synthetic was created using zero-phase wavelets. Figure 5.2 shows the extracted wavelet together with its amplitude and phase spectrum.

Figure 5.2: Extracted seismic statistical wavelet for seismic inversion analysis.

5.4 Well to Seismic Tie

White and Simm (2003) suggested some basic principles follow when seismically trying to tie.

Conditioning of well data is another safeguard. There must be no spikes in the well log data, or the real inversion results will be tampered with. The caliper log could be used as a reference log to locate washout zones and hence correct the log data.

Following the wavelet estimations, the following processes are used to correlate the well to seismic data:

- Synthetic traces are created using well data and compared to seismic traces at the well site.
- Slight squeezing and extending of the time window results in a correlation between seismic features and well.
- Between the manually adjusted well synthetic and real seismic trace, RMS error and correlation coefficient are calculated. This procedure is continued until both values are within acceptable limits.
- The correlation coefficient is 0.78 percent, which indicates a strong connection with an excellent match.
- Figure 5.3 and 5.4 shows the difference between the seismic and synthetic traces.

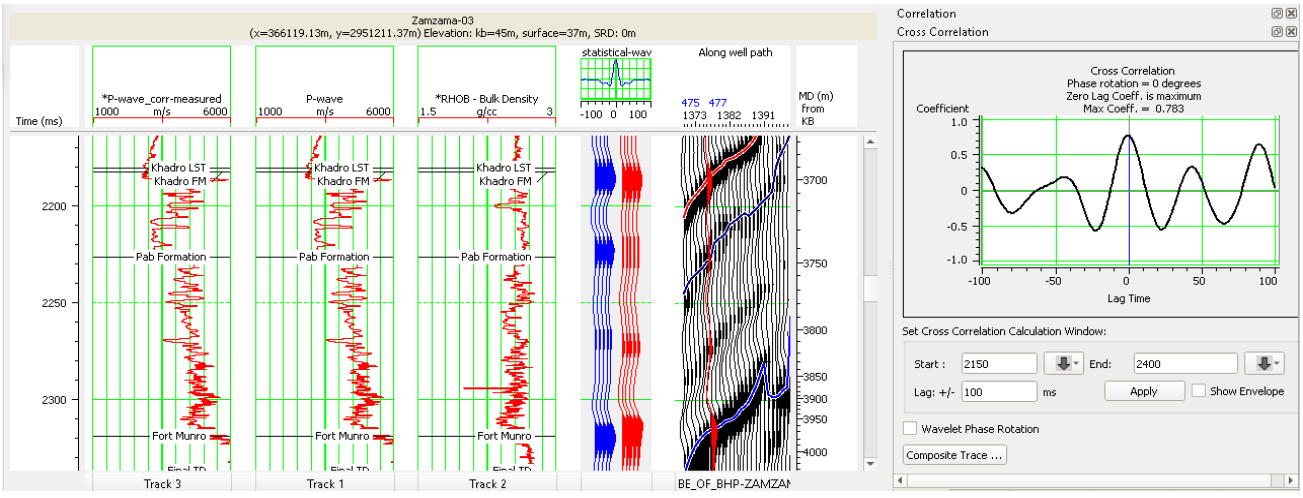

Figure 5.3 Process of seismic correlation with zamzama – 03 well log Data .

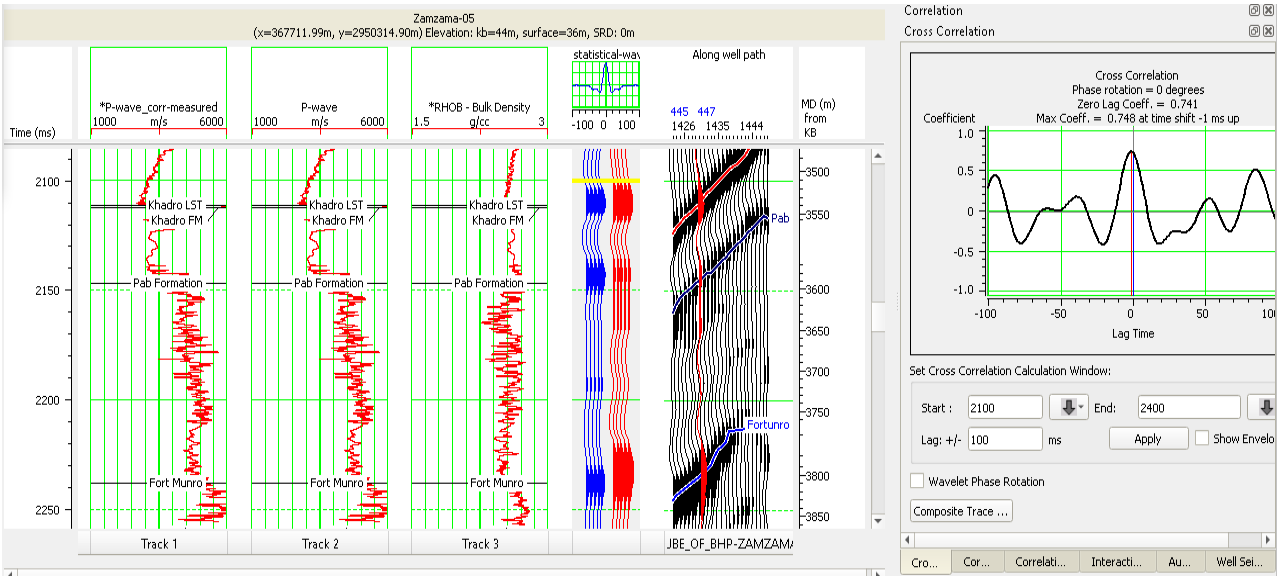

Figure 5.4 Process of seismic correlation with zamzama – 05 well log Data .

5.5 Low-frequency model

There are two types of acoustic impedance i-e absolute and relative.

"Because relative impedance is a relative property of layers and is used to determine the quantitative properties, it does not require any initial low-frequency model for its calculation" (Barclay et al., 2007). Absolute impedance is the absolute property of layers, and it is used to understand seismic data in both quantitative and qualitative ways. Inversion procedures include a frequency range of 0-15 Hz to obtain absolute impedance (Cooke and Cant, 2010). In Model-Based Inversion, low frequencies are used as part of the process.

For this investigation, a sonic log is utilized to generate low-frequency models in the neighborhood of the well. Figure 5.5 depicts a low-frequency model for inversion.

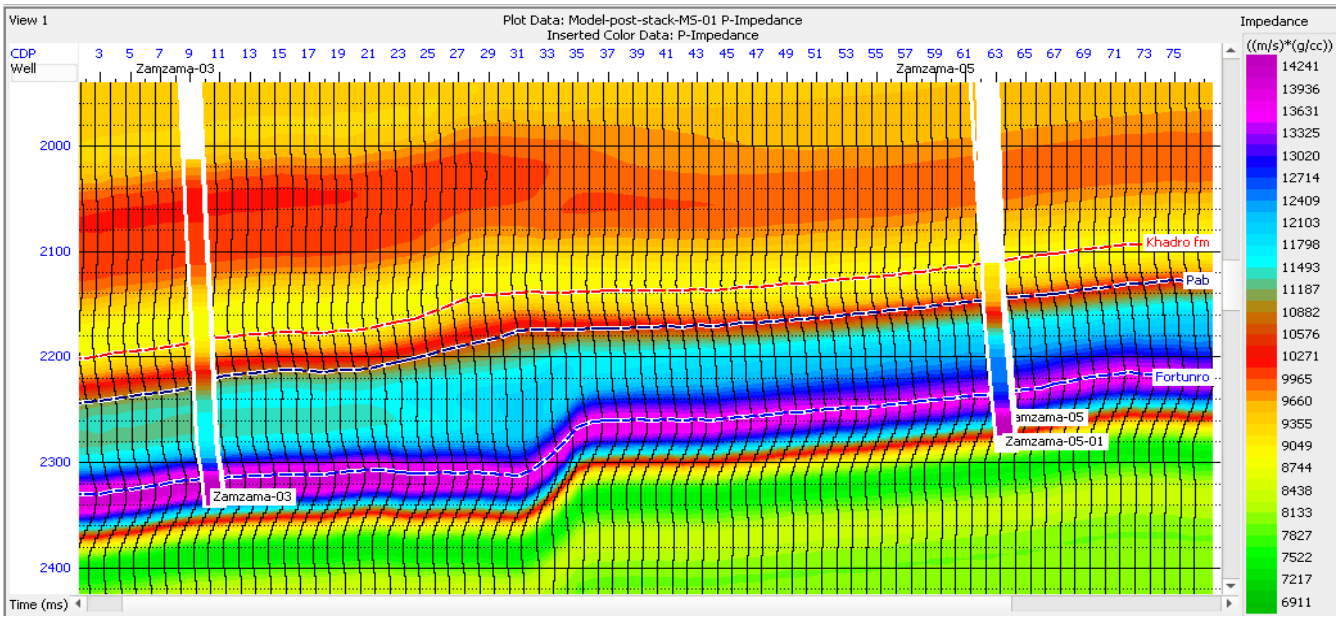

Figure 5.5: Low-frequency model used for seismic model-based inversion algorithm.

5.6 Model Based Inversion

Using convolution theory to log restricted inversion. According to the convolution theory, the normal incidence of a seismic trace can be represented by convolving the source wavelet with the earth's reflectivity and adding noise.

MBI is carried out by first creating a theoretical earth model, then comparing and updating it.

model until there is no good correlation between the synthetic seismogram and the seismic trace. It

Because seismic data cannot be inverted directly, this method is intriguing.

Because seismic data is bandlimited, Model Based Inversion is effective for thin reservoirs.

The resolution and accuracy of direct inversion approaches are insufficient to meet the exploratory requirements of a industry.

Model Based Inversion has both high and low frequency components, which is why it's so thorough.

It is possible to gather information regarding stratigraphic and physical qualities.

$$J=\text{Weight(a)}\ (St-W \otimes RC(t)) + (\text{Weight(b)})\ (M-P \otimes RC(t))$$

Where

St = Synthetic trace

W(t) = Extracted wavelet

RC(t) = Coefficient of reflectivity

P = integration operator

The integration operator P is convolved with the final reflectivity to create the final impedance, and the initial theoretical model M is the original theoretical model.

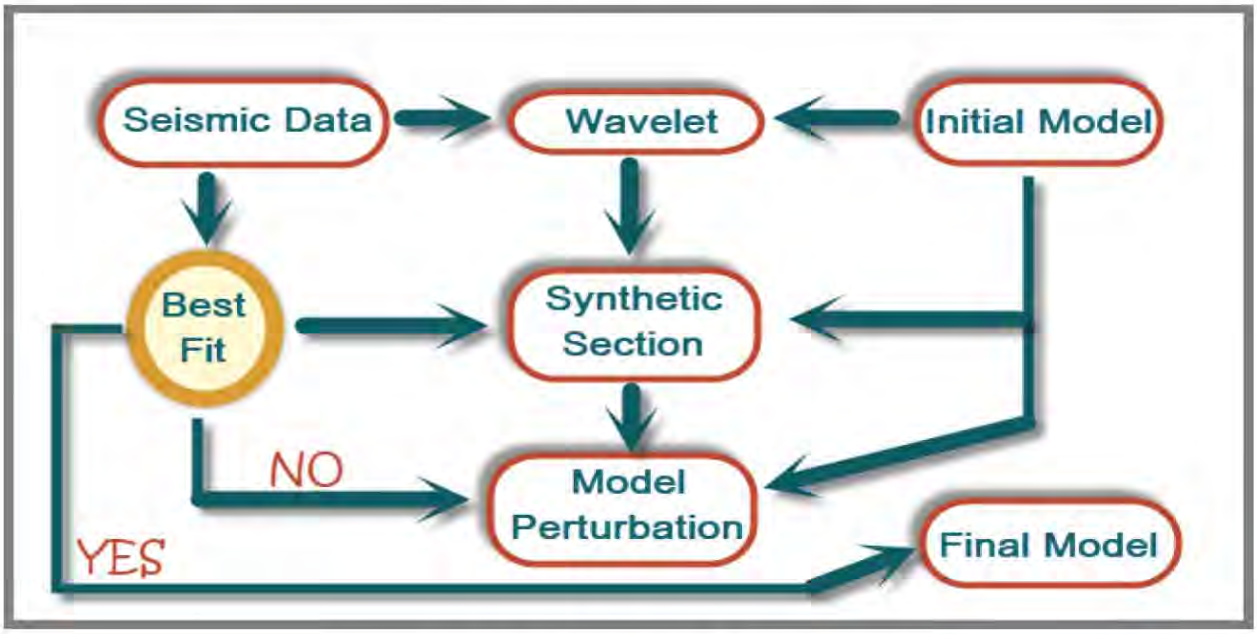

Figure 5.6: Workflow adopted for MBI

The seismic trace is modeled in the first part of the equation, and the seismic trace is modeled in the second portion.

Initially, the impedance was estimated. Figure 5.6 depicts the Model-Based Inversion workflow.

5.7 Inversion Analysis

Figure 5.7 and 5.8 shows the acoustic impedance obtained from the seismic and well log correlation. The trend of well log impedance (blue) and the correlation coefficient between seismic trace (red) and synthetic are presented in red inverted seismic impedance.

The result of the wells log (black) is 0.99, with a 0.05 % error.

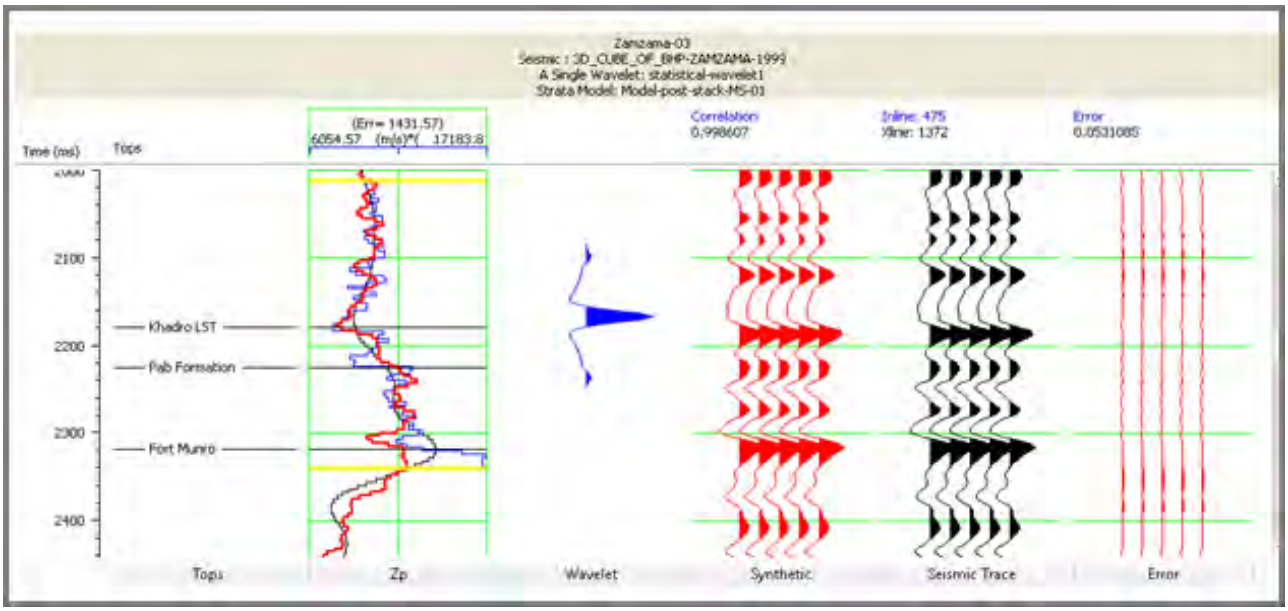

Figure 5.7: inversion Analysis of zamzama – 03

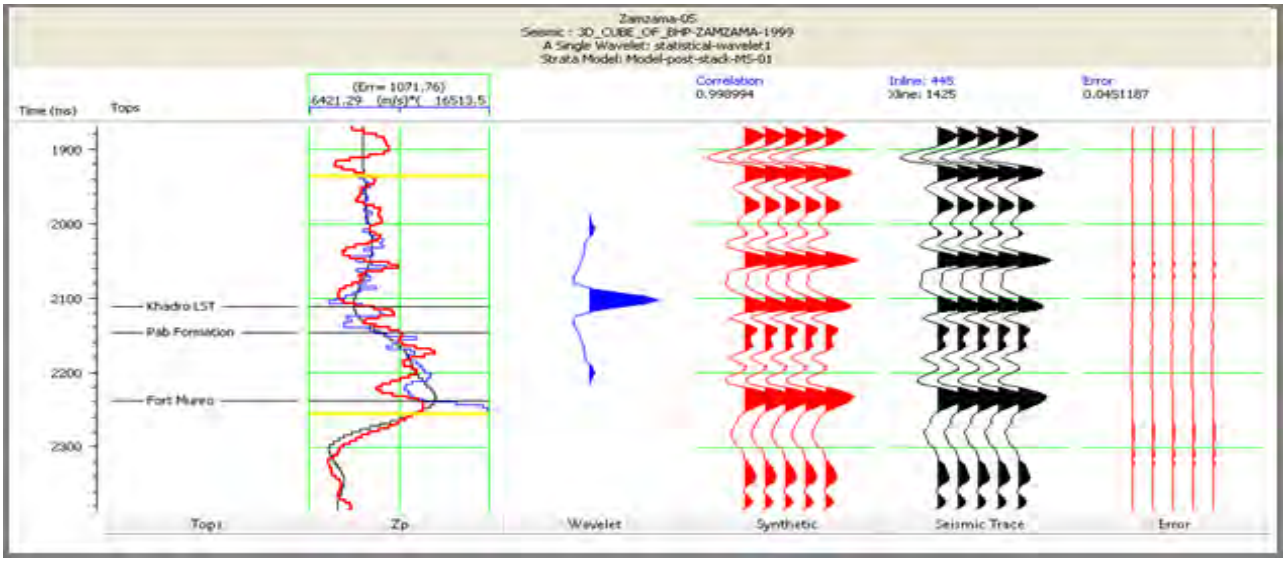

Figure 5.8: inversion Analysis of zamzama – 05

5.8 Inverted Section Zp

Model-Based Inversion was used to capture the lateral and vertical variations in acoustic impedance in the seismic region shown in Figure 5.9. Zone of Particular Interest Pab sandstone, which begins at 2200 ms and has a low impedance, indicates gas saturation.

The start of Fort Munro is characterized by a high impedance (purple) Pab sandstone base.

limestone. Model-Based Inversion has a higher vertical and lateral resolution, and it also selects the best candidate.

Within the reservoir, there is a difference in impedance. Zamzama-03 has a low impedance, as may be seen here.

This indicates that there is some low impedance activity by having saturation that can be water, oil, or gas.

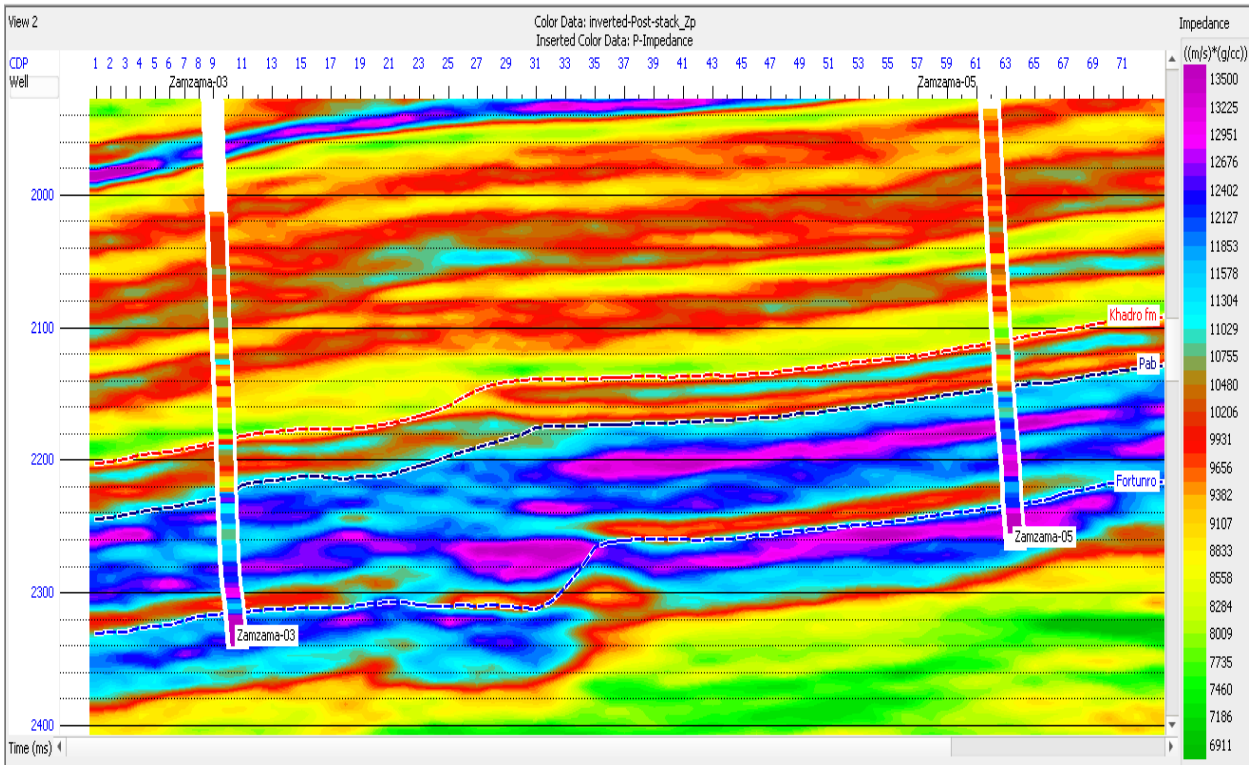

Figure 5.9: Inverted impedance of model-based inversion algorithm

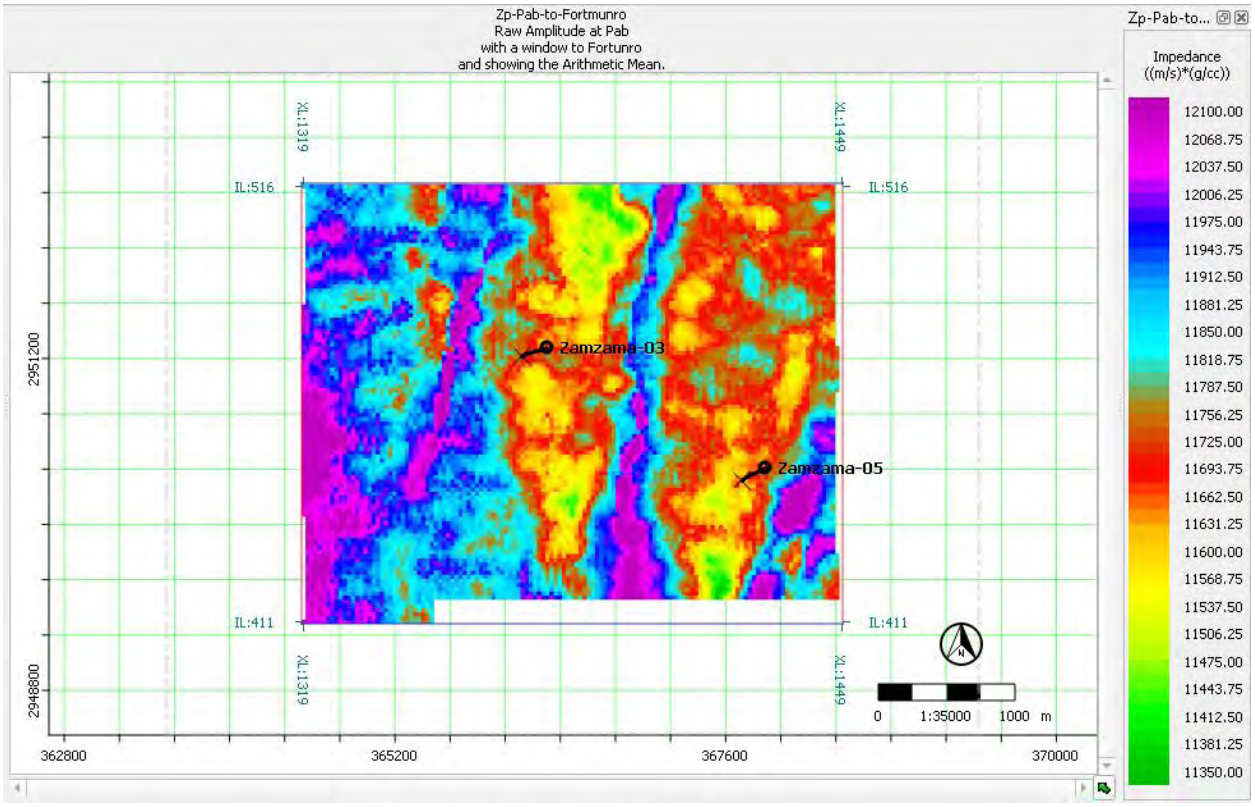

Figure 5.10: Data Slice Inverted Zp at Pab Sandstone of model-based inversion algorithm.

5.9 Cross plot

Cross plotting Vp/Vs and P-impedance with water saturation on the z-axis is used to verify feasibility. Figure 5.11 shows Vp/Vs on the y-axis, P-impedance on the x-axis.

The reservoir depth, which is Pab sand, is plotted. The Vp/Vs ratio was found to be low, ranging from 1.6 to 2.0.

The gas saturated zone with low P-impedance is highlighted in the red polygon.

While the Vp/Vs ratio is the same, the high impedance implies that some wet sands are present, as indicated by the blue polygon in both the cross plot and curve displays, as confirmed by the water saturation log displayed alongside the P-impedance.

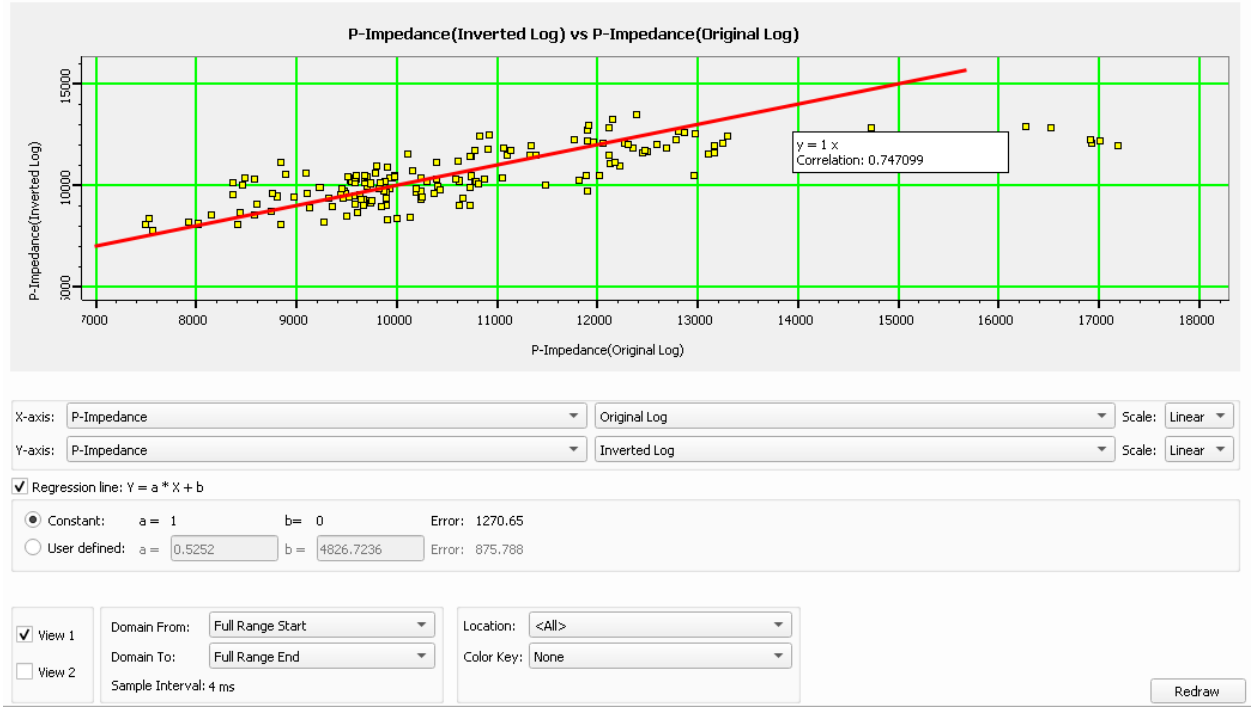

Figure 5.11: Cross-plot of Vp/Vs ratio and P-impedance and color key of Sw

5.10 Porosity Estimation

Porosity estimate requires two porosity records from distinct wells. Because they fall inside the research region, Zamzama-03 and Zamzama-05 are used for this purpose. For further processing, an inverted Zp and a specified window must be defined. Then, in a multi-attribute list, distinct attributes are selected for further results. We are given a list of estimated errors for various properties.

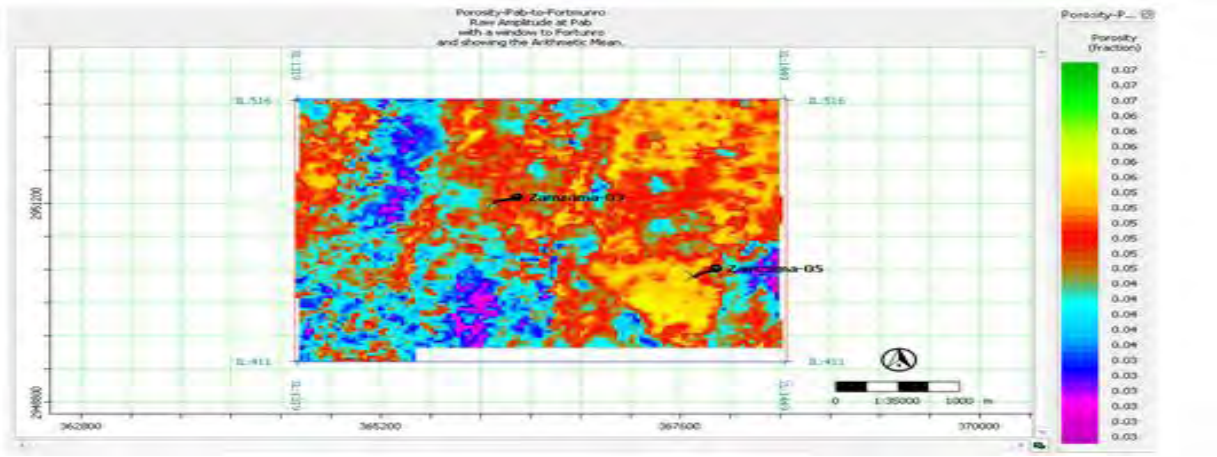

Figure 5.12: Porosity data slice at Pab

The property with the lowest inaccuracy is chosen as the one to use for porosity estimation.

In this case, a multi-attribute has run with minimal training and validation error, including time (Inverted model-based Zp), Y-coordinates (Inverted model-based Zp), derivative instantaneous amplitude, and derivative instantaneous amplitude derivative instantaneous amplitude derivative instantaneous amplitude the average number of times .

When looking at the color bar, Pab Sandstone has a porosity of 16 percent at Zamzama-03 and 9 percent at Zamzama-05. As illustrated in Figure 5.7, model-based inversion has a high correlation coefficient (of 0.99 percent) and error (0.05 percent) with seismic data. The reservoir low was resolved by MBI.

Impedance zone and has provided excellent porosity details, which are nearly identical , which was determined via petrophysical analysis .

CHAPTER#06
PROBABILISTIC NEURAL NETWORK

6.1 Introduction:

When characterizing reservoirs in shale and sandstone environments, the main challenge is locating porous and permeable formations. The modern way to address this issue is identifying seismic features linked to reservoir characterization and then combining these properties to estimate reservoir parameters (Ronghe and Korakot, 2000). These results are obtained by the application of probabilistic neural network evaluation. Once the relationship between characteristics and petrophysical properties is established, seismic attributes and impedance can be used to estimate such properties across the entire volume. As a result, it's easier to estimate lithology, fluid content, and productive zone boundaries.

A combination of the log, acoustic, and seismic features, as well as artificial neural network training, affected the technique used in this study. This research predicts porosity, lithology, and fluid content, which are subsequently used to assess the spatial extension of carbonate reservoirs and update the reservoir model (Ronghe and Korakot, 2000).

6.2 Neural networks Theory :

Neural networks can solve for multiple variables at the same time and manage the exceedingly complicated statistical analysis that is required in this case and used large volumes of seismic data to determine porosity, lithology, and water saturation, all of which are now considered geoscience challenges.

The most well-known neural network type is multi-layer feed-forward (MLF), also known as back propagation. (Although the names appear to contradict each other, they are linked by despite the fact that data is sent forward over the network, network training is done by backpropagating the error.)

The neuron is the basic unit of the MLF network, which receives data, applies a nonlinear function to it, and then outputs as the results. This is typically a sigmoidal (S-shaped) function that cycles between on and off in a circular manner and continuous decline. Even though this nonlinear concept appears straightforward now, it took scholars more than 40 years to discover it. Because of

the nonlinear structure of the neuron, this type of neural network varies from a multilinear regression (Subrahmanyam and Roo, 2008).

This nonlinearity has the potential to disclose hidden characteristics of the data, but it must be handled with attention to preventing making inaccurate predictions. In seismic analysis, there are two key applications of neural networks. The first is sample-to-sample prediction, which is when you predict something from one sample to another, and that seeks to match each sample on a three-dimensional seismic volume to a given lithological or fluid attribute, such as porosity or water saturation. When a geoscientist wishes to see how crucial reservoir parameters change at every point in a data set, sample-to-sample prediction is used (Taner, 2001).

Categorization is the second application. The goal of categorisation is to organise a group of items. At the start, the geoscientist separates the zone of interest into classes, which are then organised by the neural network throughout the seismic data volume. A method of defining categories for a specific attribute, such as porosity, such as high, mid, or low values, is called classification. Without sample-to-sample prediction, classification also gives probability or uncertainty estimates (Subrahmanyam and Roo, 2008).

The result is more geologically significant than the initial seismic inversion output in both cases. The thrust of the model is determined by the initial data's features, ground-truthing, and cross-validation. Cross-validation excludes some samples or wells from the training process, allowing the predicted values to be compared to the known (and excluded) values (Subrahmanyam and Roo, 2008).

Input seismic properties from A1 through A4 enter the input layer of the multilayer feed-forward network, which is schematically given in. In the hidden layer, neurons are represented as circles with lines signifying weight values. The value of the output is changed to match the parameter of interest in the reservoir (Sen and Stoffa, 2013).

6.3 Sample-To-Sample prediction

Training the multilinear regression or neural network at the wells is the first step in sample-to-sample prediction; the more wells, the better the output. To generate a set of properties that describe a parameter of interest, such as density, water saturation, porosity, or clay content is used.

Seismically derived attributes, such as seismic trace amplitudes or there are instantaneous phase, instantaneous frequency, and derivatives of seismic traces, as well as inversion derived properties including P-impedance, S-impedance, and density.

Although the study might employ 50 or more qualities as inputs, it has been demonstrated that this will result in "overtraining" (false prediction), hence the cross-validation technique is used to identify the statistically significant attributes, which are usually less than 10. (Taner, 2001).

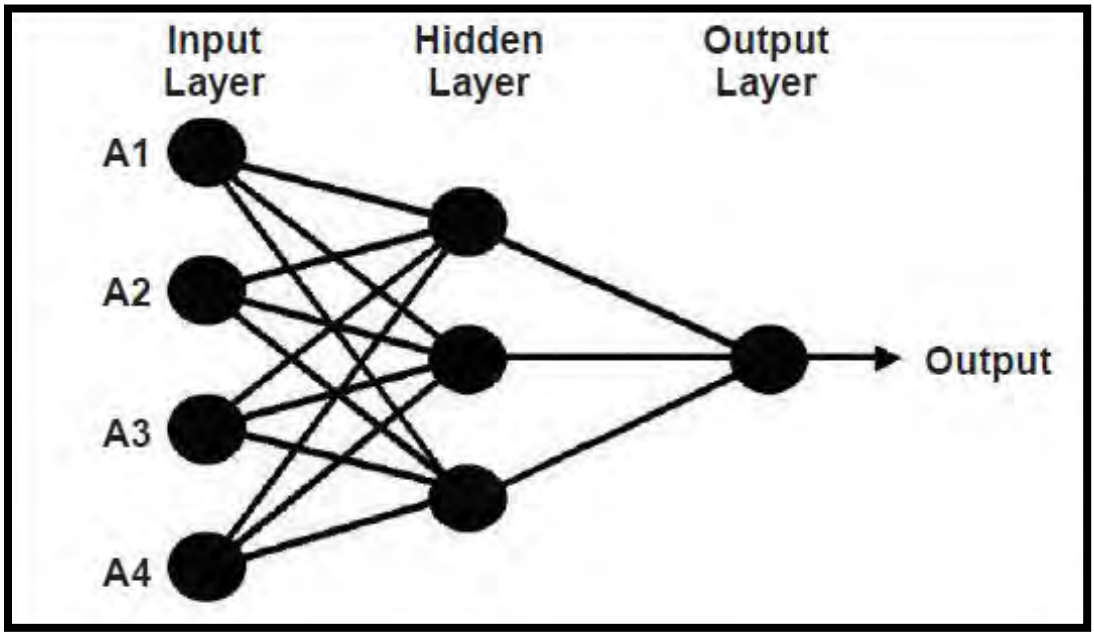

Figure 6-1 Multi-layered Feed Forward Artificial Neural Network Schematic.

Weights are allocated to the attributes after they have been chosen. In a multivariate regression technique, weights are computed using a "least-squares" method that can correct for frequency discrepancies between well and seismic measurements using a convolutional operator . A random number is commonly used as the starting weight in the neural network approach. The output obtained with these initial parameters is compared to known wells to see whether there are any differences to discover faults, which are then returned to the network to calculate a better weight for each characteristic. This repetitive training procedure's purpose is to eliminate errors and produce the best estimate of each feature across all samples in the seismic volume (Subrahmanyam and Roo, 2008).

Many statistical techniques use a least-squares strategy to reduce errors, as previously indicated. With an initial correlation that is usually very accurate, neural networks are always the preferred

option (Taner, 2001).

However, compared to linear statistical approaches, there is a far higher risk of overtraining. Cross-validation is required to determine whether the original correlation is optimal or excessive, which might lead to incorrect expectations (Taner, 2001).

6.4 Classification of Neural Network :

Classification is sometimes preferred to sample-to-sample prediction since it not only provides information on specific features of interest, but also the likelihood of their occurrence in any given portion of the seismic data (Nizam and Zhang, 2020).

First, the asset team must determine which classes they wish to focus on. The neural network must be trained to distinguish the classes after they have been defined. Training dates back to the early days of brain research, when scientists were attempting to recreate human learning. That learning comes from experience, and in the geoscience industry, experience with accounting difficulties comes from wells. Because wells are supposed to provide more information than seismic, this is the case (Nizam and Zhang, 2020).

On the other hand, the well data is far less than the seismic data. As a result, geoscientists train seismic to provide the most accurate well fits possible. The sample-to-sample technique's training and prediction provide the geoscientist with a best-fit solution but no confidence estimations. As previously said, categorization is unique in that it provides us with a confidence, or probability, estimate (Russell, 2006).

6.5 Non-Linear Regression with Multiple Attributes (Probabilistic Neural Network)

Since the 1980s, artificial multi-layer feed-forward neural networks have been utilised to solve a variety of geophysical problems. Working with high-quality seismic and well data is appropriate for a probabilistic neural network. The probabilistic neural network does not require knowledge of the seismic wavelet and does not rely on an input forward model. Its stability is higher than that of a multi-layer feed-forward neural network. (Russell, 2006).

A probabilistic neural network is a mathematical interpolation method that is implemented using a three-layered feed-forward neural network design. During training, each training node is only

visited once. The training data log values are believed to be a linear combination of the output target log values. Figure 6.2 depicts the fundamental construction of a Probabilistic Neural Network (Nizam and Zhang, 2020).

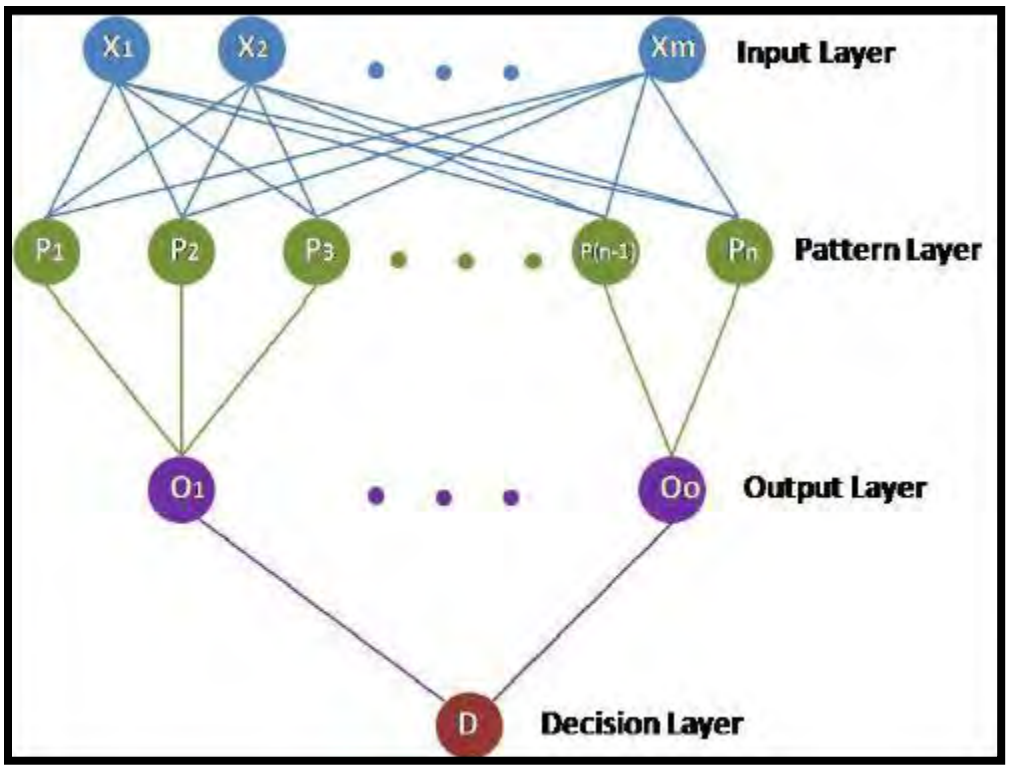

Figure 6-2 Basic design of a Probabilistic neural network (Subrahmanyam and Roo, 2008).

The validation error is the sum of all hidden wells' prediction errors. The validation issue occurs when the PNN is applied to the entire volume of seismic data. When employed as PNN inputs, multiple qualities may be geologically disturbing; numerous attributes may be statistically significant but lack theoretical justifications (Rijks and Jauffred, 1991). Multi-attribute data must be viewed in the context of a geologic skeleton, not a statistical one. Results that are geologically reasonable and physically feasible are necessary to be reliably used for exploration and exploitation purposes (Nizam and Zhang, 2020).

6.6 Procedure

The purpose of this study is to discover a nonlinear operator that can forecast well logs based on seismic data features. The logs for the wells are estimated using this operator after the operator has been calculated. The attribute volumes and cross-sections are mapped using these projected logs (porosity, volume of shale, and fluid saturation).

It uses contain

- Post-stack seismic volume data in 3D.
- A network of wells used to connect seismic data. Each well has a "target log" that contains data like porosity, gamma rays, and water saturation that can be forecast for other sites. Determine that each well includes shot-corrected sonic logs for converting depth to time.
- (Optional) The data contains one or more "external" attributes in the form of seismic 3D volumes. The analysis is limited to internal features that can be inferred from raw seismic data in the absence of such attributes.

6.7 Internal Attributes

An internal seismic property is any mathematical transformation of seismic trace data. Examples of simple features are instantaneous phase, instantaneous frequency, trace envelope, and so on (Hampson-Russell Manual).

6.8 External Attributes

External attributes, such as Impedance and AVO properties, cannot be estimated within the seismic trace data context. In addition to seismic trace data, other data sources, such as seismic trace inversion, may be employed in this calculation (Hampson-Russell Manual).

6.9 When determining the Target Log, Attributes are employed.

Other attributes are employed in place of raw seismic data since the analysis demands a nonlinear linear relationship between the quality, which may show nonlinear activity and so improve the technique's prediction power. The characteristics will be nonlinear, which will improve the technique's ability to predict. Another reason is that it is frequently beneficial to break down input data into its constituent parts. This approach called preprocessing or feature extraction can greatly improve the pattern recognition system by reducing the dimensionality of the data before using it to train the system. Preprocessing can also be used to add prior information into a pattern recognition system's architecture.

Fitting a curve through a group of points is similar to this procedure. When you add an attribute, it's the same as mounting the polynomial order.(Hampson-Russell Manual).

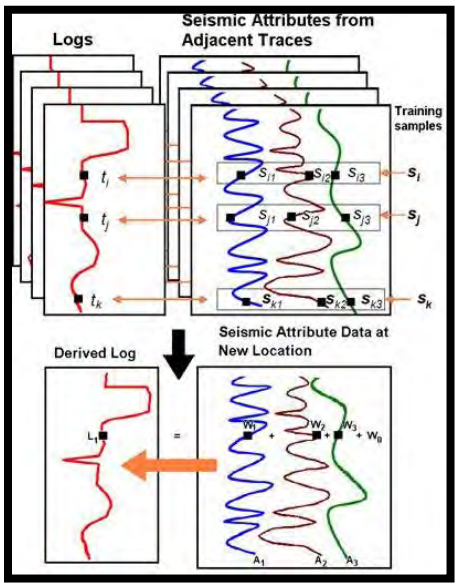

Figure 6-3 The log data was preprocessed to decrease its dimensionality (Rijks and Jauffred, 1991).

6.10 Mathematical Explanation

The problem is solved using a non-linear neural network. The prediction power and resolution of computed attribute volumes can be improved. A probabilistic neural network was utilised in this study, which is similar to the interpolating technique.

Assume we know the exact values of three seismic qualities' needed characteristics.

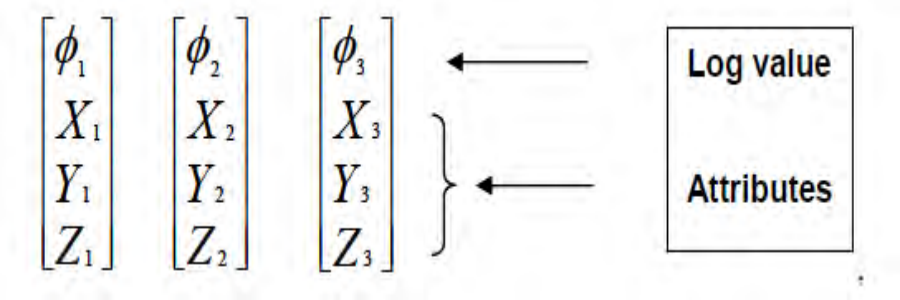

The objective is to find a new output point:

$$\begin{bmatrix} ? \\ X_0 \\ Y_0 \\ Z_0 \end{bmatrix}$$

By comparing the new property to the known attributes, the problem is solved. The predicted value in a probabilistic neural network is a linear combination of the known training values.

$$\phi_0 = w_1 * \phi_1 + w_2 * \phi_2 + w_3 * \phi_3$$

Where:

* Is the convolution

φ is the porosity value

wi are the weights

The primary disadvantage of a probabilistic neural network is that it takes a long time to apply because it carries all training data and compares each output sample with each training sample (Hampson-Russell manual).

6.11 Emerge Training Data

The Emerge process aims to bring together well log and seismic data. The general purpose is to use seismic data features to predict a well log property. Any measurable log type, such as porosity, or a determined lithologic attribute, such as shale volume, maybe that characteristic. In Emerge training, seismic, impedance, and well data are loaded.

6.12 Reservoir Properties Prediction by Neural Network

The Hampson-Russel in the Emerge module is used to predict porosity using a neural network. To execute the Probabilistic neural network, certain steps must be followed. Figure 6.4 illustrates the details of these steps.

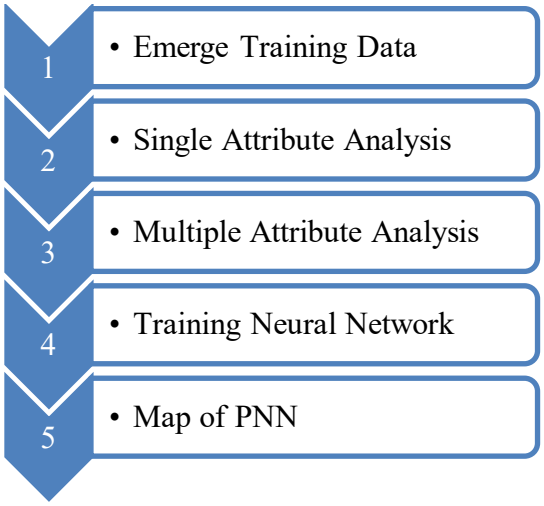

Figure 6-4 Workflow of Probabilistic Neural Network.

6.13 Training Neural Network

To increase target prediction, Emerge Neural Network capabilities were used. Because of this, the non-linear features of the Neural Network will improve both the predictive power and the resolution of the resulting target volume.

Emerge contains four methods under the topic of Neural Network:

1. Probabilistic (PNN).
2. Multi-layer Feed Forward (MLFN).
3. Discriminant Analysis.
4. Radial Basis Function (RBF).
5. Convolutional (CNN).

The Discriminant analysis algorithm is not a Neural Network, but we have put it in this group because of its classification capabilities. Our main interest in the algorithms listed above is the Probabilistic Neural Network. For the PNN multi-attribute selection procedure, the attributes that are best for predicting the target log have been determined. By selecting a different amount of characteristics (known as Integrated Absolute Amplitude), you can create a Neural Network with the same attributes as the transform.

When compared to multi-attribute regression, the correlation is significantly higher. This is typically the case with Neural Networks due to the non-linear structure of the operator. It's also important to note that the Neural Network was only used during the training windows. This is done for two reasons: first, it saves time i-e

The application time can be significant if the Neural Network is applied to the entire window.

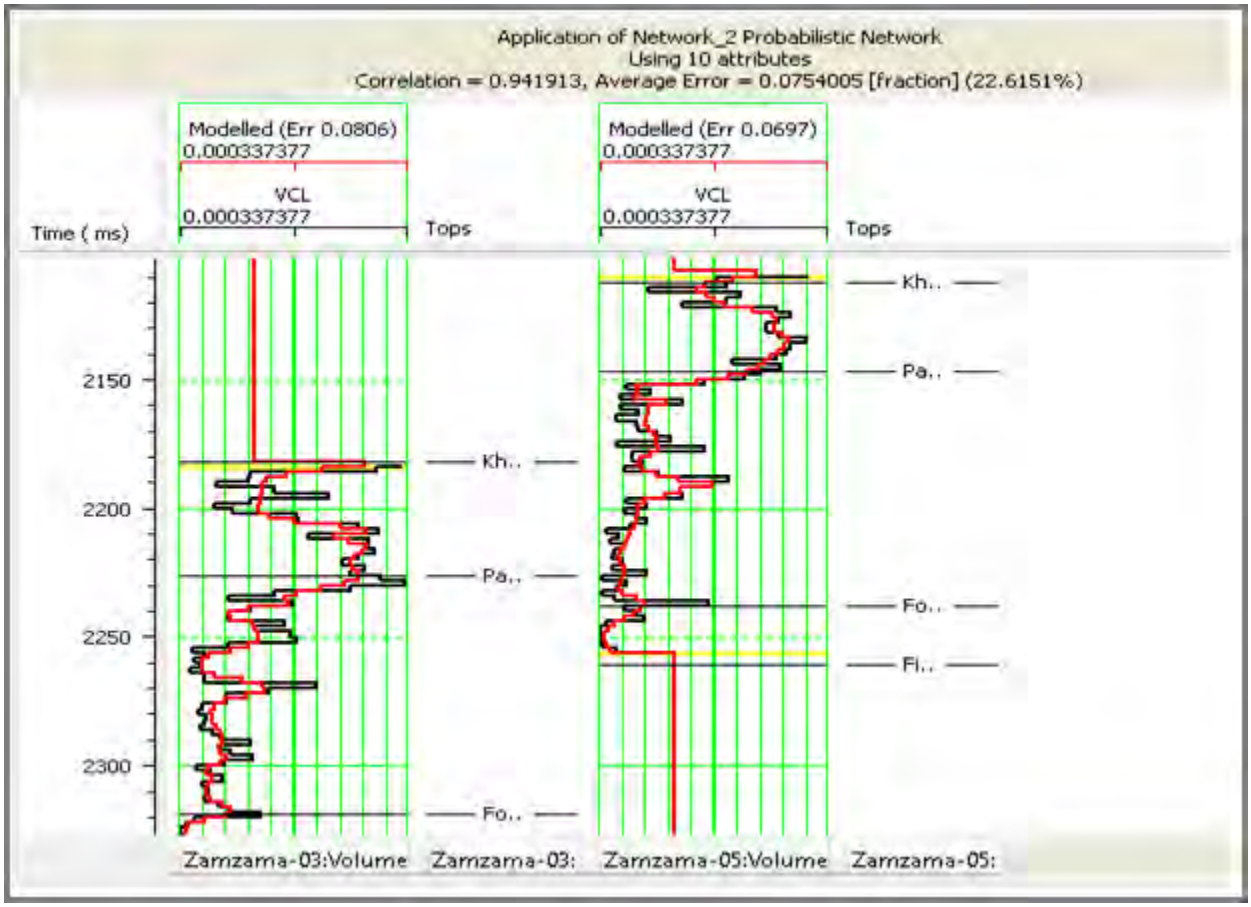

Figure 6-5 Probabilistic neural network result on volume of shale.

And secondly, The Neural Network has a hard time extrapolating beyond the constraints of the training data. As a result, it's likely to be less accurate than multi-linear regression outside of the training windows.

Figures 6.5,and 6.6 show the results of the Probabilistic Neural Network, which indicate that the amount of shale, and average porosity are all good. The correlation is 94.1 percent, and 93.3 percent, for the volume of shale, average porosity, accordingly by using different Seismic

attributes i-e time, phase, Amplitude, frequency etc. For each reservoir property, twenty different characteristics are run since the best result for correlation is required for reservoir properties with the least amount of inaccuracy. To establish an excellent correlation, more qualities can be run. The correlation result is 94.1 percent for the volume of shale, 93.3 percent for average porosity with the error of 0.075, and 0.012 correspondingly.

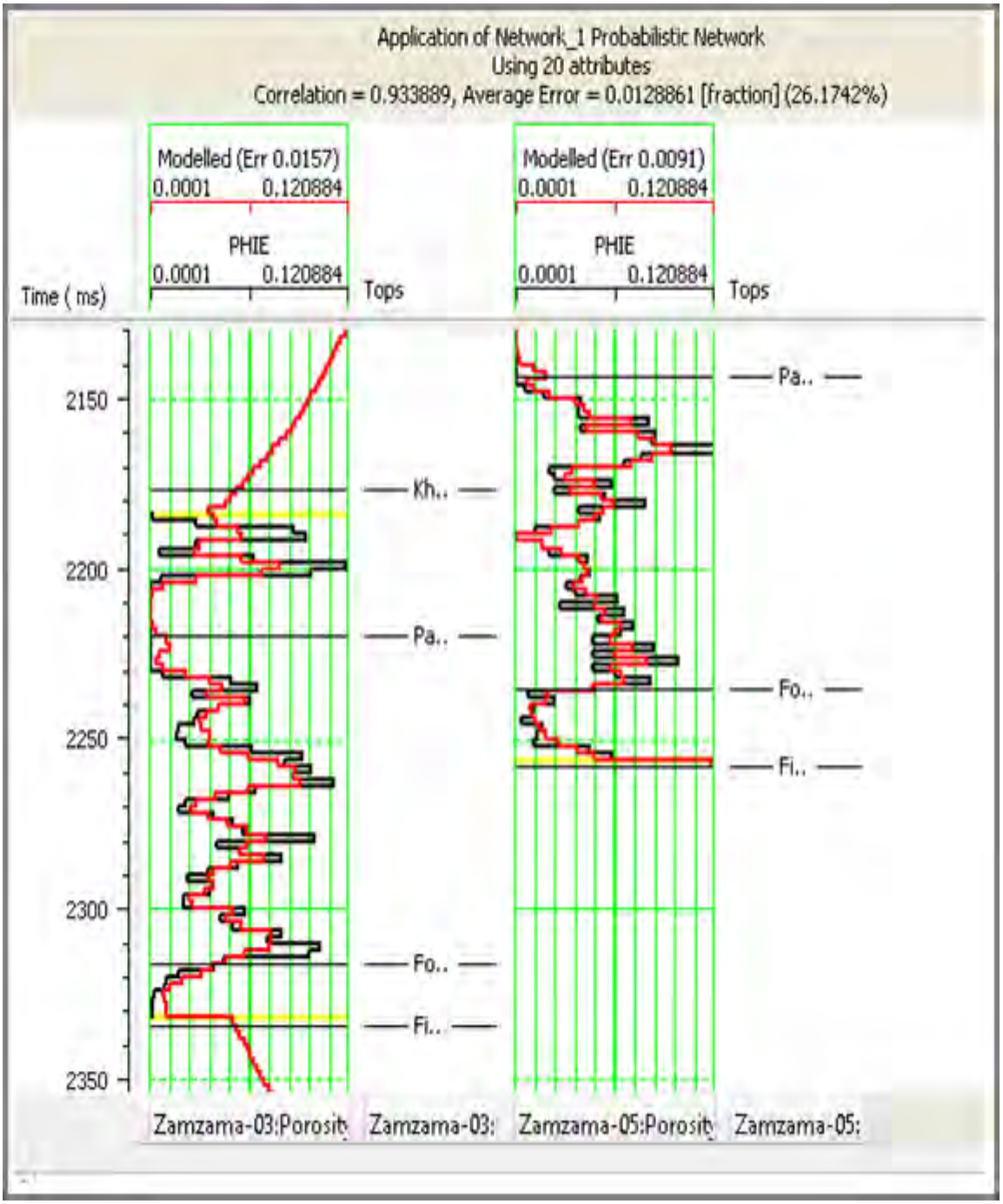

	Target	Final Attribute	Training Error	Validation Error
1	Porosity	Integrated Absolute Amplitude(inverted-Post-stack_Zp)	0.031135	0.032247
2	Porosity	Instantaneous Frequency	0.029750	0.031262
3	Porosity	Filter 35/40-45/50	0.029154	0.030819
4	Porosity	Filter 5/10-15/20	0.028603	0.035129
5	Porosity	Dominant Frequency	0.027641	0.092937
6	Porosity	Apparent Polarity	0.026931	0.127948
7	Porosity	Apparent Polarity(inverted-Post-stack_Zp)	0.026567	0.119561
8	Porosity	Amplitude Envelope(inverted-Post-stack_Zp)	0.026259	0.120337
9	Porosity	Second Derivative	0.025969	0.113819
10	Porosity	Integrate(inverted-Post-stack_Zp)	0.025386	0.113182
11	Porosity	Time	0.025095	0.178579
12	Porosity	Average Frequency(inverted-Post-stack_Zp)	0.024324	0.279904
13	Porosity	Instantaneous Phase(inverted-Post-stack_Zp)	0.023663	0.126798
14	Porosity	Amplitude Weighted Phase(inverted-Post-stack_Zp)	0.023053	0.123496
15	Porosity	Filter 45/50-55/60(inverted-Post-stack_Zp)	0.022829	0.088766
16	Porosity	Integrate	0.022529	0.178174
17	Porosity	Integrated Absolute Amplitude	0.022317	0.164032
18	Porosity	Amplitude Weighted Frequency(inverted-Post-stack_Zp)	0.022110	0.161583
19	Porosity	Instantaneous Frequency(inverted-Post-stack_Zp)	0.021867	0.152670
20	Porosity	1/(inverted-Post-stack_Zp)	0.021690	0.163669

Figure 6-6 Probabilistic neural network result on average porosity by using 20 Seismic attribute.

6.14 Cross plot

After you've finished with the neural network, you'll need to create a probabilistic neural network cross plot. The actual and expected reservoir properties are plotted in cross plots. Actual values are plotted on the X-axis, while predicted values are plotted on the Y-axis. Figures 6.7,and 6.8 show a cross plot of the actual and predicted volume of shale and average porosity, respectively.

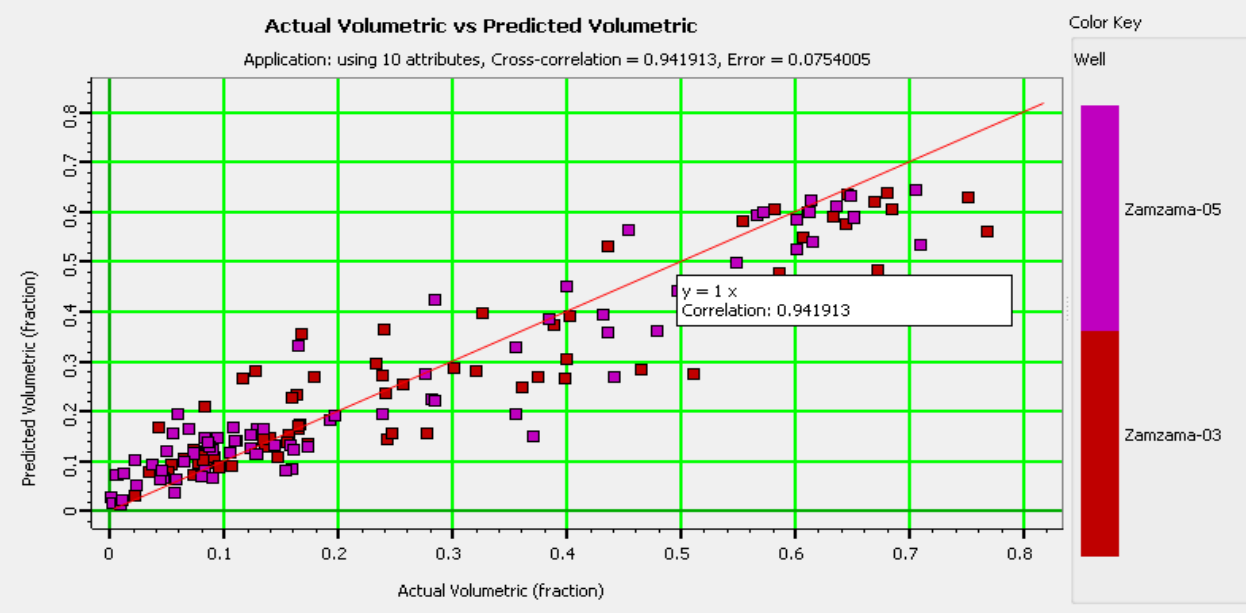

Figure 6-7 Cross plot actual volume of shale vs predicted volume of shale.

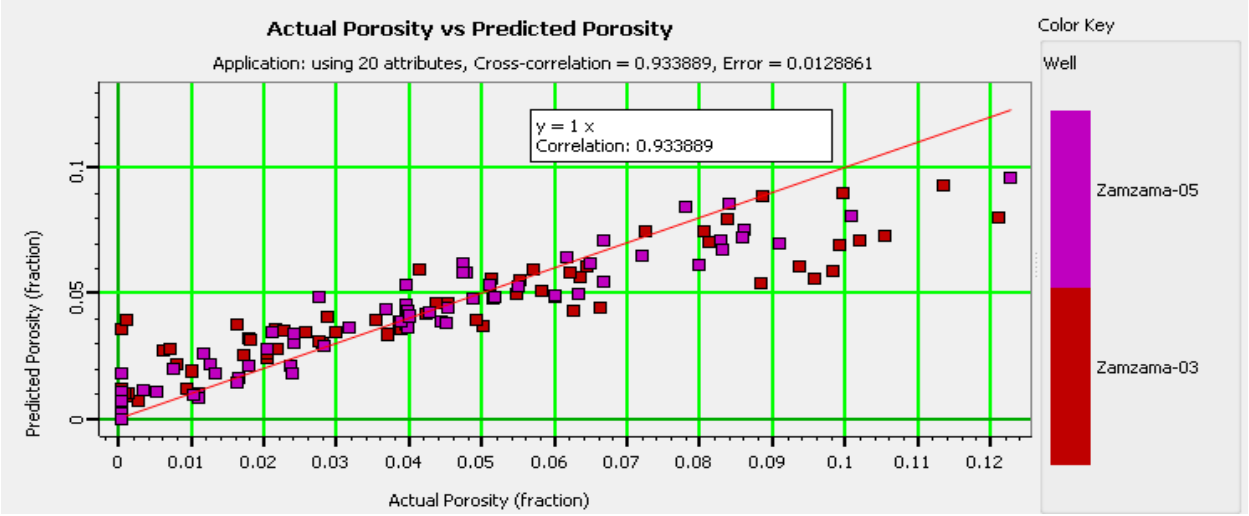

Figure 6-8 Cross plot actual average porosity vs predicted average porosity.

6.15 Slices

Finally, the results of Probabilistic neural networks are loaded into a three-dimensional seismic cube of impedance datasets to determine the overall variation in shale volume and porosity . After cutting the slices, the results are compared to the petrophysics results to determine the exact parameters.

6.16 Volume of Shale

On the Khadro and Pab Sandstone formations, volume shale slices are run. The general trend of the Pab Formation figure 6.9 and 6.10 is that there is less shale volume on the west side of the slices, more shale volume on the middle portion of the slices, and then less shale volume on the east side.

Furthermore, the numbers obtained from slices are compared to petrophysical results to get the most accurate shale volume estimation. Table 6.1 compares the results of both neural network and petrophysical studies in terms of shale volume. The change in shale volume in Khadro and Pab Sandstone slices is shown in Figures 6.9 and 6.10. The center area of the map in Khadro shows a higher volume of shale, while the western and eastern sides show lesser values. A larger shale volume was detected at the well location in Pab.

Table 6-1 Comparing the result of Neural and Petrophysical analysis of volume of shale.

Volume of Shale		
Zamzama 3		
Formations	Neural network	Petrophysical Analysis
Pab	35% (average)	30-35%
Zamzama 5		
Formations	Neural network	Petrophysical Analysis
Khadro	60 % (average)	38 %
Pab	45 % (average)	47 %

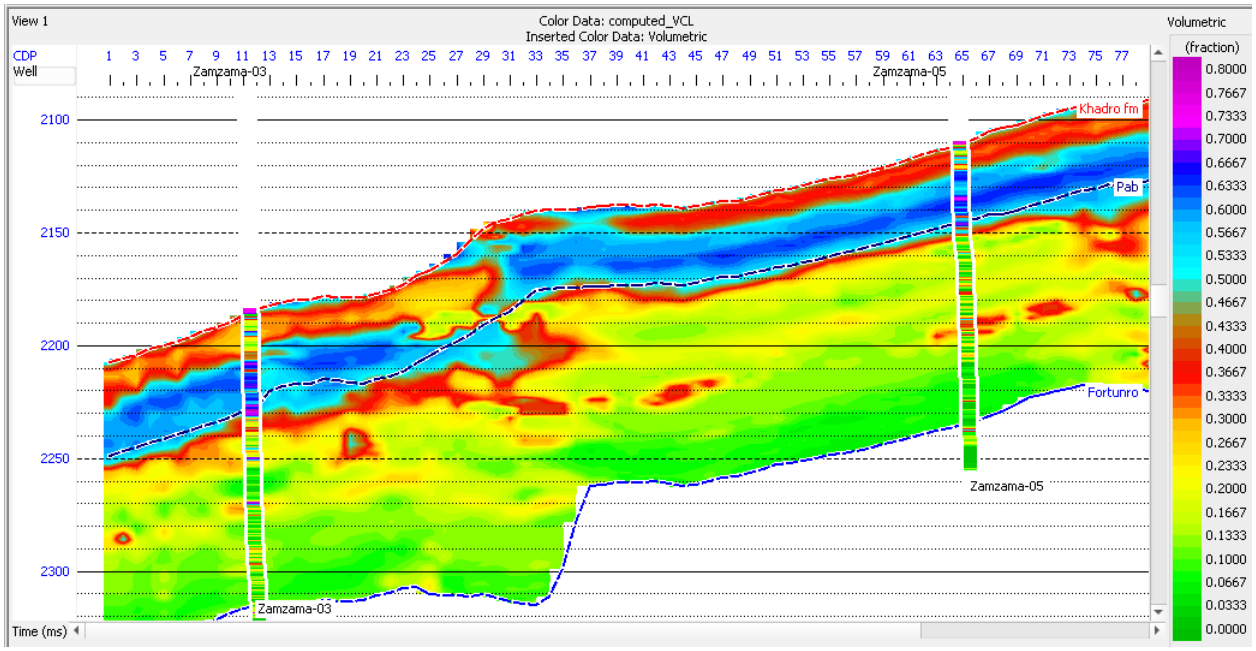

Figure 6-9 Probabilistic Neural network estimation of volume of shale for Pab Formation.

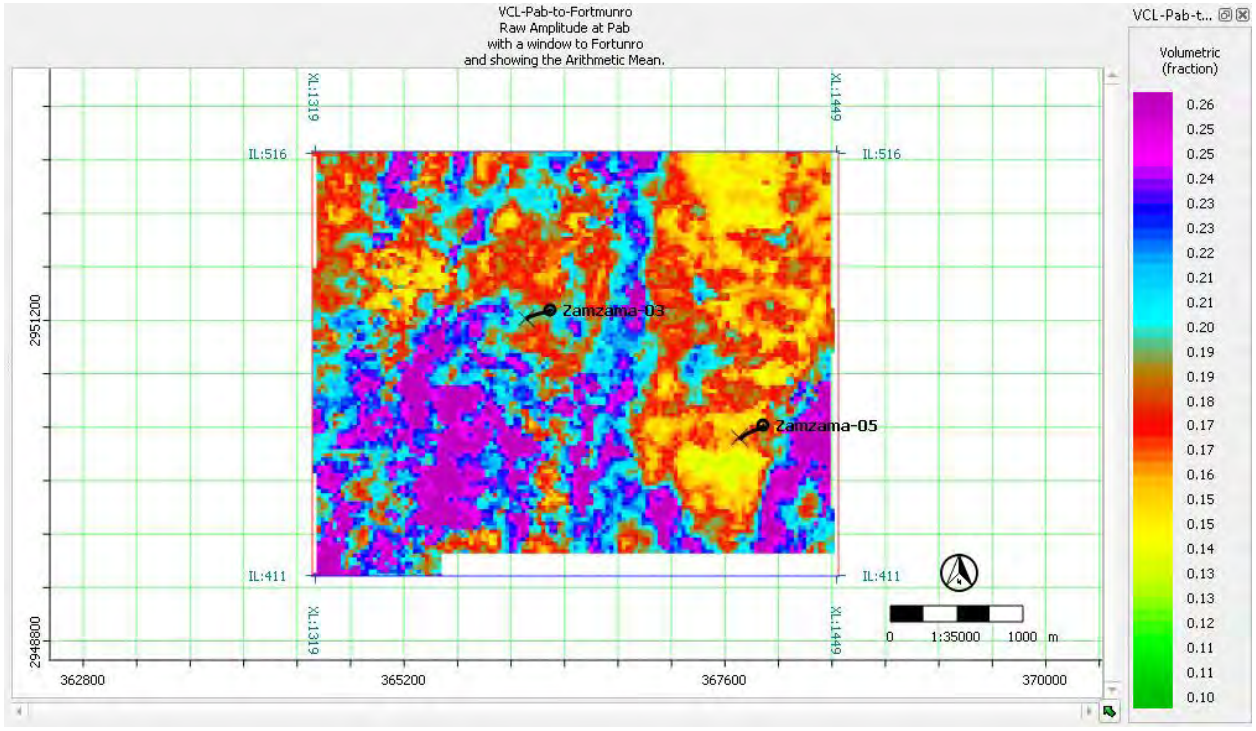

Figure 6.10 Avg slice of volume of clay

6.17 Average Porosity

On the Khadro and Pab Sandstone formations, average porosity slices are taken. Figure 6.11 shows the general trend of the Pab Formation, which shows a mixed variation of porosity in the entire slice with a range of 10% to 20%. Figure 6.12 shows a significant fluctuation in porosity in the Pab Sandstone Formation. Near the well Zamzama 3 and Zamzama 5 , the porosity increases, while the porosity decreases when we move away . Pab Sandstone has a porosity range of 10% to 18%.

In addition, the values obtained from slices are compared to the petrophysical results to provide the most accurate estimate of average porosity. The comparison of the results of porosities obtained by neural network and petrophysical analysis is provided in table 6.2.

Table 6-2 Comparing the result of Neural and Petrophysical analysis of average porosity.

Average Porosity		
Zamzama 03		
Formations	Neural network	Petrophysical Analysis
Pab	21	14
Zamzama-05		
Khadro	14	13.5
Pab	16	15

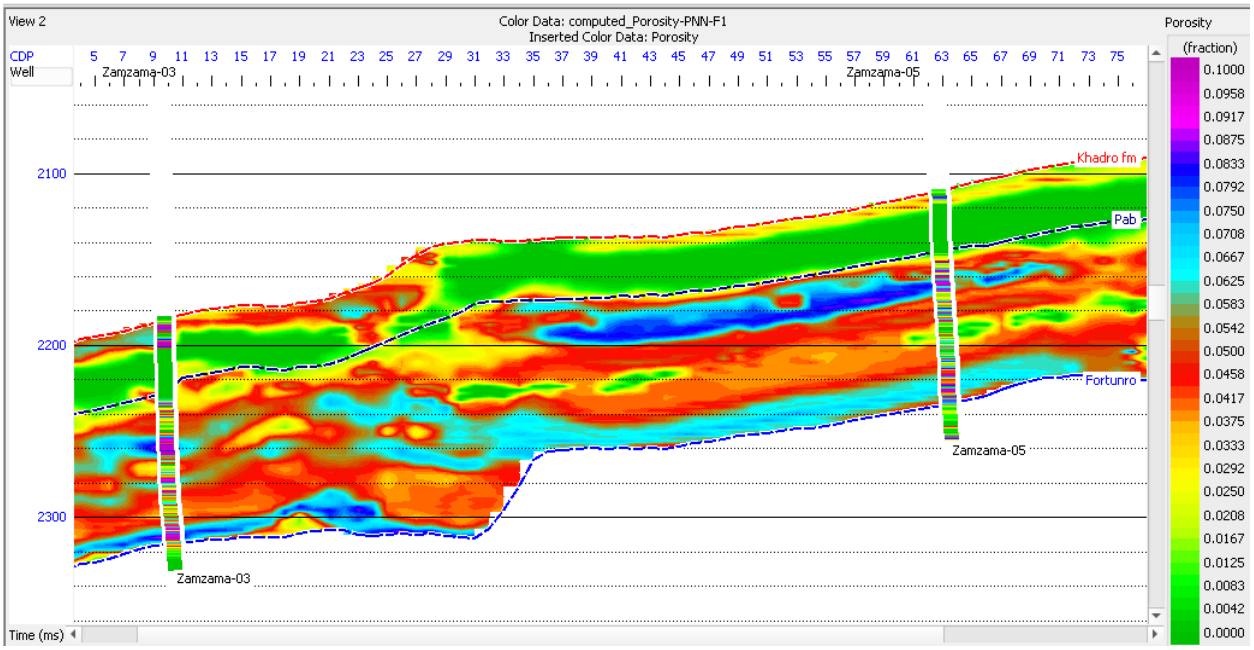

Figure 6-11 Probabilistic Neural network estimation of average porosity for Pab Sandstone Formation.

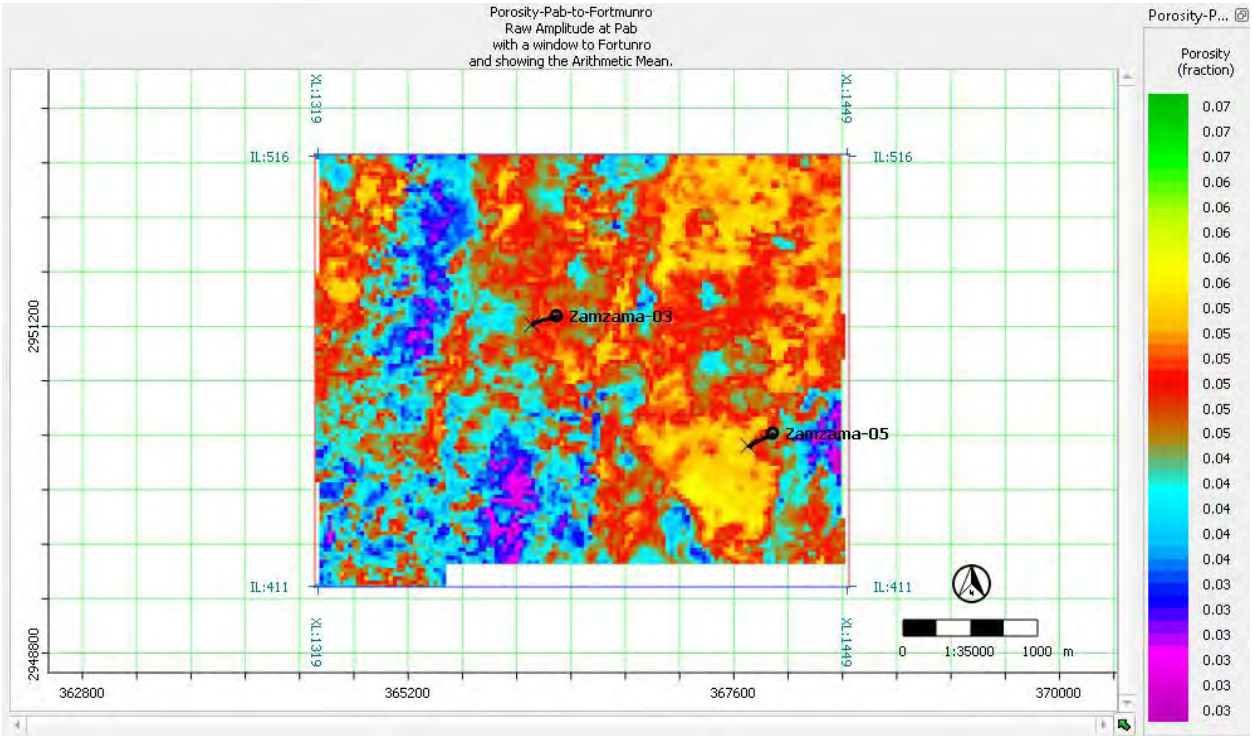

Figure 6.12 Avg slice porosity of pab fm

PNN's results for shale volume, and porosity show a strong correlation with Petrophysical analysis. The petrophysical parameters of the Zamzama Block can be more accurately estimated using the PNN approach.

Conclusions:

Interpreted seismic section of study area reveals compressional regime which shows thrusted anticlinal structure, also confirmed by time and depth contour maps. Major lithology in Zamzama Gas field is Sand with interbedded shale is confirmed by facies analysis. Petrophysical results confirms reservoir potential of Pab sandstone at Zamzama 03 well with 10-20% PHIE, 10-30% Sw and 70-90% Hydrocarbon saturation. Comparative study of inversion algorithms (by using 3D seismic data of Zamzama area along with two well log Data) suggests that MBI has more reliable results in study area have showing low impedance contrast in many area . And than by performing PNN to predict seismic reservoir properties from well log data and seismic attributes like (Time, Amplitude, Phase, frequency etc) by using Hampson Russell software .

REFERENCES:

- Abbasi, S. A., Asim, S., Solangi, S. H., & Khan, F. (2016). Study of fault configuration related mysteries through multi seismic attribute analysis technique in Zamzama gas field area, southern Indus Basin, Pakistan. Geodesy and Geodynamics, 7(2), 132-142.

- Ahmed Abbasi, S., Asim, S., Solangi, S. H., & Khan, F. (2016). Study of fault configuration related mysteries through multi seismic attribute analysis technique in Zamzama gas field area, southern Indus Basin, Pakistan. Geodesy and Geodynamics, 7(2), 132–142. https://doi.org/10.1016/j.geog.2016.04.002 .

- Asquith, G. B., Krygowski, D., & Gibson, C. R. (2004). Basic well log analysis (Vol. 16). Tulsa: American Association of Petroleum Geologists.

- Asquith, G. B., Krygowski, D., & Gibson, C. R. (2004). Basic well log analysis (Vol. 16). Tulsa, OK: American association of petroleum geologists.

- Bacon, M., Simm, R., & Redshaw, T. (2003). 3-D seismic interpretation. 3-D Seismic_Interpretation(First).Cambrige.University.Press.https://doi.org/10.1017/CBO9780511 802416.

- Bacon, M., Simm, R., & Redshaw, T. (2007). 3-D seismic interpretation. Cambridge University Press.

- Badley, M. (1985). Practical Seismic Interpretation. Badley, Ashton, and Associates Ltd. https://doi.org/10.1029/EO067i047p01342-06 .

- Barclay, F., Bruun, A., Rasmussen, K. B., Alfaro, J. C., Cooke, A., Cooke, D. A.Roberts, R. (2007). Seismic Inversion: Reading Between the Lines. Oilfield Review .

- Bhpbilliton. (2003). THE ZAMZAMA FIELD,Pakistan, 12–15 .

- Bust, V. K., Majid, A. A., Oletu, J. U., & Worthington, P. F. (2013). The

petrophysics of shale gas reservoirs: Technical challenges and pragmatic solutions. Petroleum Geoscience, 19(2), 91-103.

- Coffeen, J. A. (1986). Interpreting seismic data .
- Cooke, D., & Cant, J. (2010). Model-based seismic inversion: Comparing deterministic and probabilistic approaches. CSEG Recorder, 35(4), 29-39.
- Cosgrove et al., (1998) , Advances in the study of Fractured Reservoirs .
- Daniel, (2003) , Basic Well log Analysis .
- Donaldson, T. &. (2015). Petrophysics (Fourth). Gulf Professional Publishing .
- Dorn, R.I. (1998) Rock Coatings. Elsevier, Amsterdam, New York, 429 p.
- Dorn, R.I., (1998). Digital processing of back-scatter electron imagery: a microscopic approach to quantify chemical weathering. Geological Society of America Bulletin 107, 725– 741.
- E.Badley, M. (1987). Practical Seismic Interpretation. Badley, Ashton, and Associates Ltd. https://doi.org/10.1029/EO067i047p01342-06.
- FatmiA.N.,Iqbal.,M.W.A,Raza.,H.A.,andRaza,S.M., (1972), Stratigraphy of Pakistan, Shah,S.M.I, edition, Geological Survey of Pakistan ,Memoirs,v.12:Quetta,Geological Survey of Pakistan,137p.
- Haas and Dubrule, (1994) , Geostatistical inversion; Seismic data po reservoir properties .
- Hampson – Russell Manual (tutorial)
- (Jackson et al., 2007) Aitchison, J., & Wardaugh, R. (1987). An Introduction to Sociolinguistics. In The British Journal of Sociology (Vol. 38, Issue 3). https://doi.org/10.2307/590702 .

- Jackson, M., Jellis, R., Hill, R., Roberson, P., Woodall, M., Wormald, G., & Jafri, N. (2007). Zamzama Gas Field - Balancing Risk and Value. Society of Petrolium Engineers, 1–12. https://doi.org/10.2523/88577-ms .
- Kadri, I. B. (1995). Petroleum Geology of Pakistan: Pakistan Petroleum Limited. Karachi, Pakistan.
- Kamel and Mabrouk, (2002) , A Modified Approach for Volumetric Evaluation of Shaly Sand Formations from Conventional Well Logs:
- Kazmi, A. H., & Jan, M. Q. (1997). Geology and tectonics of Pakistan. Graphic publishers.
- Kearey Philip. (1988). An introduction to Geophysical Exploration (Third). John Wiley & Sons. https://doi.org/10.1016/j.jafrearsci.2017.04.031 .
- Krygowski, (2003) , Guide To Petrophysical Interpretation .
- (Nizam et al., 2020) glacial surface organic carbon in the Western Himalaya .
- Pendrel, J., (2000), Seismic inversion – a critical tool in reservoir characterization. Scandinavian Oil-Gas Magazine, 5/6
- Qadri, I. B. (1995). Petroleum geology of Pakistan. Pakistan Petroleum Limited.
- Raza, H.A, Ali, S.M, Riaz, A., (2002), Petroleum Geology of Kirthar sub basin and Part of Kutch basin Pakistan. Journal of Hydrocarbon research.no.1, 29-73.
- Rider, M. (1995). The Geological Interpretation of Wells Logs (Secound). Gulf Pub Co.
- Rijks And Jauffred (1991) , An important application in any detailed 3-D interpretation study .
- Ronghe and Korakot, (2000) , Acoustic impedance interpretation for sand distribution adjacent to a rift boundary fault .

- Russell, B. (2006). Seismic Inversion Analysis. Society of Exploration Geophysicists, 876–878.
- Schlumberger, (1989), Log Interpretation/charts: Houston, Schlumberger Well services,Inc.
- Sen, and stoffa M. K. (2013). Seismic inversion (1st ed.). Richardson, TX.: Society of Petroleum Engineers.
- Sen, M. K. (2006). Seismic inversion (1st ed.). Richardson, TX.: Society of Petroleum Engineers.
- Sheriff, R. E., (1999), Inferring stratigraphy from seismic data: AAPG Bulletin, v. 60, p. 528-542.
- Subrahmanyam and Roo, (2008) , Application Of Artificial Neural Networks .
- Taner, M.T., (2001), Seismic Attributes, CSEG Recorder, p.48-56.
- Veeken & Da Silva, (2004) , Data Conditioning for a Combined Inversion and AVO Reservoir Characterisation Study .
- Zaigham, N. A., & Mallick, K. A. (2000). Prospect of hydrocarbon associated with fossil-rift structures of the southern Indus basin, Pakistan. AAPG bulletin, 84(11), 1833- 1848.